3B2v8.06a/w (Dec 5 2003).51c + model | YJTBI : 4256 | Prod.Type:FTP pp.1–22(col.fig.:NIL) | ED:S.AmjadP PAGN:ashok SCAN:manjula

ARTICLE IN PRESS

Available online at www.sciencedirect.com

SCIENCE DIRECT®

Journal of Theoretical Biology ▮ (▮▮▮▮) ▮▮▮–▮▮▮

Journal of Theoretical Biology

www.elsevier.com/locate/yjtbi

Mathematical modeling of humoral immune response suppression by passively administered antibodies in mice

Dokyun Na, Dongsup Kim, Doheon Lee*

Department of BioSystems, KAIST, 373-1 Guseong-dong Yuseong-gu, Daejeon 305-701, Republic of Korea

Received 26 October 2005; received in revised form 2 January 2006; accepted 17 January 2006

Abstract

Although passively administered antibodies are known to suppress the humoral immune response, the mechanism is not fully understood. Here, we developed a mathematical model to better understand the suppression phenomena in mice. Using this model, we tested the generally accepted but difficult to prove "epitope masking hypothesis." To simulate the hypothesis and clearly observe masking of epitopes, we modeled epitope-antibody and epitope-B-cell receptor interactions at the epitope level. To validate this model, we simulated the effect of the antibody affinity and quantity as well as the timing of administration on the suppression, and we compared the results with experimental observations reported in the literature. We then developed a simulation to determine whether the epitope-masking hypothesis alone can explain known immune suppression phenomena, especially the conflicting results on $F(ab')_2$ fragment-induced suppression, which has been shown to be no suppression, or similar to or up to 1000-fold weaker than the suppression by intact antibody. We found that suppression was caused by a synergistic effect of both epitope masking and rapid antigen clearance. Although the latter hypothesis has lost support because FcγRI/III mutant mice show antibody-mediated suppression, our simulations predict that, even in FcγRI/III mutant mice, the immune response can be suppressed according to the antibody affinity. Our model also effectively reproduced the conflicting results obtained using $F(ab')_2$ fragments. Thus, in contrast to the idea that the $F(ab')_2$ results prove the FcγRIIb involvement in suppression, our mathematical model suggests that the epitope-masking hypothesis together with rapid antigen clearance explains the conflicting results.

Keywords: Immune suppression; Mathematical model; Antibody; Epitope masking

1. Introduction

The humoral immune response can be suppressed by passively administered antibodies (Tao and Uhr, 1966). A classical example of this is Rhesus prophylaxis (Chilcott et al., 2003; Clarke et al., 1963; Kumpel, 2002; Moise, 2002), wherein a Rh^- woman, lacking D-antigen on her erythrocytes, can develop antibodies against D-antigens acquired from her Rh^+ child. In a subsequent pregnancy, these antibodies can be produced and damage Rh^+ erythrocytes of her fetus. For Rhesus prophylaxis, anti-D-antigen antibodies are administered, which prevent the adverse immune response. More recent applications of antibody-mediated immune suppression include transplantation across discordant blood types using anti-CD20 antibodies (e.g. rituximab) to inhibit antibody-mediated rejection (Aggarwal and Catlett, 2002; Bourget et al., 1995; Golay et al., 2000; Warren et al., 2004) or the dampening of inflammation by altering macrophage cytokine production through passively administered antibodies (Anderson et al., 2002).

Although antibody-mediated immune suppression has been successfully applied in clinical situations, the underlying mechanism of suppression is still under debate. Three hypotheses have been proposed to explain the suppression. The first hypothesis, called "epitope masking", claims that B cells are prevented from stimulation through the B-cell receptor (BCR) due to a reduction of available antigenic determinants by passively administered antibodies. Consequently, B cells are no longer stimulated so that the B-cell

*Corresponding author. Tel.: +82 42 869 4316; fax: +82 42 869 4310.
E-mail addresses: dkna@bisl.kaist.ac.kr (D. Na), kds@kaist.ac.kr (D. Kim), dhlee@biosoft.kaist.ac.kr (D. Lee).

0022-5193/$ - see front matter © 2006 Published by Elsevier Ltd.
doi:10.1016/j.jtbi.2006.01.019

population decreases (Cerottini et al., 1969; Heyman, 2001, 2003; Karlsson et al., 2001a; Möller and Wigzell, 1965; Quintana et al., 1987; Tao and Uhr, 1966). The second hypothesis is called "Fc receptor-mediated suppression" (Heyman, 1990, 2003). In this case, antigen bound to the BCR activates the tyrosine-based activation motifs in the intracellular domain of the BCR (Cambier, 1995). When activated, this domain mediates further signaling by recruiting protein tyrosine kinases (PTK) containing SH2 domains (Reth et al., 1991). The antigen–antibody complex, however, mediates crosslinking of the BCR and FcγRIIb on the B-cell membrane by binding to both the BCR and FcγRIIb. While BCR recognizes the corresponding antigen, FcγRIIb binds to the Fc part of the antibody. In this case, the PTK bound to BCR does not trigger an activation signal, but activates the nearby immunoreceptor tyrosine-based inhibitory motif, an intracellular domain of FcγRIIb. When this domain is activated by tyrosine phosphorylation, it recruits SH2-containing protein tyrosine phosphatases such as SHIP or SHP-2, which inhibit intracellular signaling (Brauweiler et al., 2001; Ravetch and Lanier, 2000; Sármay et al., 1999). The result is that B-cell activation is inhibited but apoptosis is induced (Ashman et al., 1996). The third hypothesis for suppression is that the antigens are rapidly eliminated; administered antibodies bind to antigens, after which the antibody-coated antigens are eliminated by FcγR$^+$ cells via phagocytosis before the antigens can stimulate B cells (Heyman, 2003).

Although observations from human interventions tend to support the FcR-mediated suppression hypothesis, experimental results from mice support the epitope masking hypothesis (Kumpel and Elson, 2001). Furthermore, results from human experiments cannot be explained by the epitope masking hypothesis. For example, occupation of only 8–20% of D-antigens by anti-D antigen antibodies is sufficient for suppression (Kumpel et al., 1995). In brief, occupation of 200–400 out of 10^4 D-antigens per red blood cell (RBC) is enough to suppress the humoral immune response (Kumpel and Elson, 2001). In addition, antibody binding to *K* antigen on RBCs suppresses the immune response to D-antigen in D$^-$K$^-$ humans immunized with D$^+$K$^+$ RBCs (Woodrow et al., 1975). Immune suppression in humans is all or none, and is not induced by IgE, an antibody type not recognized by FcγRIIb (Finn et al., 1961).

As mentioned above, experimental results from mice support the epitope masking hypothesis rather than FcγRIIb-mediated B-cell inhibition or FcγRI/FcγRIII-mediated rapid clearance of antigen via phagocytosis. It is thought that FcγRIIb, which recognizes the Fc part of IgG, does not play a crucial role in immune suppression because suppression by IgG is unaltered by the loss of FcγRIIb (Heyman et al., 2001; Karlsson et al., 2001b). Also, administered antibodies normally suppress the B-cell response even in FcγRI$^{-/-}$ or RcγRIII$^{-/-}$ mice, which lose their phagocytotic ability (Barnes et al., 2002; Karlsson et al., 1999, 2001a). In addition, the immune response is suppressed not only by IgG but also by IgE and IgM, which cannot be recognized by FcγR (Brüggemann and Rajewsky, 1982; Cerottini et al., 1969; Heyman and Wigzell, 1984; Karlsson et al., 1999, 2001a). Suppression can also be induced by F(ab′)$_2$ fragments lacking the Fc part, although they also fail to induce suppression (Brüggemann and Rajewsky, 1982; Enriquez-Rincon and Klaus, 1984; Heyman, 1990) or are less effective than intact antibody (Cerottini et al., 1969; Karlsson et al., 1999; Tao and Uhr, 1966). Other experimental results also support the idea that suppression is not mediated by Fc receptors but rather by masking of epitopes in mice. For instance, compared to human rhesus prophylaxis, 1000 times more antibody is required for effective suppression in mice (Kumpel, 2002; Kumpel and Elson, 2001). Also, suppression can be altered by the timing of antibody administration or by changes in antibody affinity, and the degree of suppression is quantitatively related to the amount of antibody administered (Karlsson et al., 1999, 2001b).

Although the epitope-masking hypothesis has garnered more support in mice, there have also been some conflicting results, especially in studies using F(ab′)$_2$ fragments. In complex systems, such as the immune system, mathematical models are very useful for testing competing hypotheses (Merrill, 1998). They are especially helpful for determining the validity of the epitope masking hypothesis because it is difficult to prove experimentally (Heyman, 2003). Therefore, in the current studies, we developed a mathematical model to help clarify the immune suppression by passively administered antibodies in mice. We then validated the model by comparing in silico results with experimental results from the literature.

In this report, we first describe the relevant biological background and previously developed mathematical models. We then explain why our model is based on the clonal expansion model rather than other advanced models, and we discuss differences between our model and conventional clonal expansion-based humoral immune models. After describing the model in detail, we validate it by comparing the results of the simulation with experimental results obtained from the literature. Finally, we investigate our model in silico using parameters obtained from the literature to answer whether the epitope masking hypothesis alone can explain the immune suppression, why F(ab′)$_2$ fragment and intact antibody experiments often show different results in spite of equivalent affinities, and whether the different results can be explained by the epitope masking hypothesis.

2. Relevant background

The humoral immune response is initiated upon recognition of antigens by B cells. B cells take up the antigens and present them on their surface (Bonnerot et al., 1995; Patel and Neuberger, 1993). Primed Th cells, which already recognize the antigen, then bind to the presented antigen fragments via the T-cell receptor and send a signal that

induces the proliferation of B cells for the production of plasma cells or for the generation of centroblasts to form germinal centers (McHeyzer-Williams et al., 2001). The plasma cells initially produce IgM antibodies and then switch to downstream isotypes, including IgG, IgA, or IgE (McHeyzer-Williams et al., 2001; Tarlinton, 1998). In the germinal center, B cells produced from the centroblast mutate their antigen recognition genes, a process called somatic hypermutation (Kimoto et al., 1997; Wilson et al., 1998). Mutant B cells with low or no affinity die due to a failure to recognize antigens harbored by follicular dendritic cells or to receive signals from Th cells (Cozine et al., 2005). The germinal center plays a role in the generation of plasma cells with switched isotypes, but its main purpose is to generate high-affinity memory B cells for the secondary immune response (Cozine et al., 2005; Guzman-Rojas et al., 2002; Han et al., 1997; Kevin Hollowood, 1998; Maclennan, 1994; McHeyzer-Williams et al., 2001; Tarlinton, 1998).

A number of mathematical models have been developed to better understand the humoral immune response. The earliest models were developed by Bell and were based on a prey-predator system and clonal expansion theory (Bell, 1970a, b, 1971a, b). The models were further advanced by incorporating a threshold for the initiation of B-cell proliferation (Waltman and Butz, 1977) or by introducing replicating antigens for B-cell stimulation (Merrill, 1978a, b). The models were also advanced by incorporating not only clonal expansion but also isotype switching, germinal center reactions, memory B-cell formation, and Th-dependent B-cell priming processes (Beck, 1981; Bocharov and Romanyukha, 1994; Funk et al., 1998; Keşmir and De Boer, 1999; Pierre et al., 1997; Rundell et al., 1998).

3. Mathematical model

We developed a mathematical model based on the clonal expansion of B cells. We did not incorporate germinal center reactions, Th cell-dependent B-cell priming, or isotype switching from IgM to IgG in our model. The germinal center first appears around 4–5 days after immunization (Han et al., 1997; Kevin Hollowood, 1998; Liu et al., 1991; Maclennan, 1994; McHeyzer-Williams et al., 2001), but the immune response is substantially suppressed by administered antibodies within 5 days post-immunization (Heyman and Wigzell, 1984; Karlsson et al., 1999, 2001a, b; Möller and Wigzell, 1965). Thus, the suppression is not associated with germinal center reactions. In addition, the primary immune suppression is generally considered in the context of immune suppression in mice. Therefore, we focused the model on the primary immune response and did not incorporate the germinal center reactions. In the case of Th-dependent B-cell priming, it has been reported that administered antibody does not interfere with Th priming or Th-dependent B-cell priming (Karlsson et al., 1999).

In the immune response against sheep red blood cells (SRBCs), plasma cells secrete IgM for up to 5 days and then switch to IgG (Strasser et al., 1991; Yoshii et al., 1996). The primary difference between IgM and IgG is not in their ability to bind to antigens but rather in their Fc part (Kracker and Radbruch, 2004). Due to IgM's pentameric structure, it covers more epitopes than IgG, but IgM is degraded seven times more rapidly than IgG (Junghans and Anderson, 1996). During the immune response, far more antibodies are produced than antigens (Bachmann et al., 1994; Leanderson et al., 1992). Consequently, the ability of IgM and IgG to eliminate antigens does not differ significantly. In addition, according the epitope masking hypothesis, differences in the constant region of the antibody do not affect immune suppression (Brüggemann and Rajewsky, 1982; Cerottini et al., 1969; Heyman and Wigzell, 1984; Karlsson et al., 1999, 2001a). Thus, we treated both IgM and IgG as 'antibody' without distinction.

Although our model is based on clonal expansion, it has three differences from the previous clonal expansion-based models. First, we included the apoptosis of B cells upon loss of the antigenic signal via the BCR (Donahue and Fruman, 2003; Pittner and Snow, 1998; Rathmell, 2004) because activated B cells not generated from the germinal center can be also induced to undergo apoptosis (Donahue and Fruman, 2003). Second, we developed the model at the epitope level to investigate the effects of administered antibodies on epitope masking. For instance, in the model, we considered individual epitope interactions with the antibody or BCR, and B-cell stimulation and survival were dependent not on the antigen concentration but rather on the concentration of available unmasked epitope. Third, we incorporated organ-level antigen sequestration in the model. Because SRBCs are used to study immune suppression in mice, we also used SRBCs as an antigen in our model. Unlike pathogenic antigens, injected SRBCs are captured mainly in the liver and spleen by macrophages (Guo et al., 2000; Ouchi et al., 1976; Rihova and Vetvicka, 1984; van Rijen et al., 1998). In the liver, this involves elimination of senescent RBCs by specialized macrophages, called Kupffer cells, whereas in the spleen, it involves trapping of pathogens and induction of an immune response (Naito et al., 1997). Because the elimination of SRBCs by Kupffer cells in the liver is a natural mechanism for clearing RBCs and not an immune-inducing mechanism (Naito et al., 1997), we divided the model organism into three compartments: an antibody injection site (blood), an immune-inducing organ (spleen), and a non-inducing organ (liver) (Fig. 1).

This model, however, is limited because it does not considering spatial hindrance between antibodies for binding to epitopes. Due to the larger size of the antibody compared to the epitope, bound antibody can prevent nearby epitopes from being recognized by other antibodies. Such spatial hindrance explains the non-epitope-specific suppression: an antibody suppresses not only its corre-

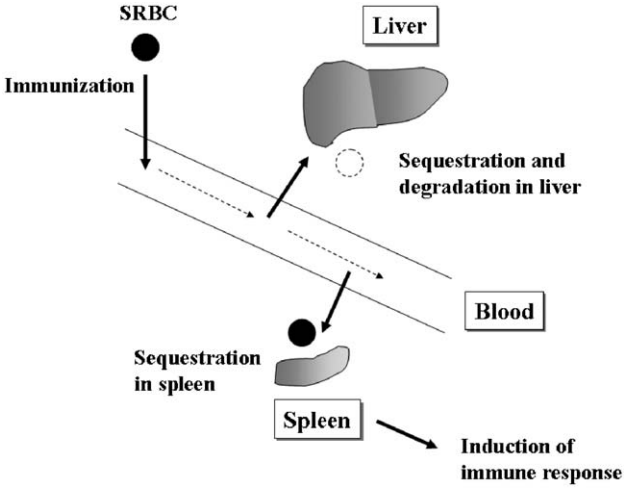

Fig. 1. SRBC sequestration at an organ level. SRBCs injected into blood are trapped and eliminated by macrophages in the liver (e.g. Kupffer cells), which degrade SRBCs, or they can be trapped in the spleen by immune cells, inducing an immune response.

sponding epitope-specific immune response but also responses to other epitopes on the same antigen. Because of this limitation, we did not investigate the non-epitope-specific suppression phenomenon.

The ordinary differential equations are listed below. Variables and parameters are briefly described in Tables 1–4. The units of the variables are "numbers", for instance the number of B cells, the number of produced antibodies, the number of SRBCs, or the number of administered antibodies or $F(ab')_2$ fragments.

3.1. Overview of model equations

$$\frac{dS_{blood}}{dt} = -\rho_{liver}S_{blood} - \rho_{spleen}S_{blood}, \quad (1)$$

$$\frac{dS_{spleen}}{dt} = \rho_{spleen}S_{blood} - \delta S_{spleen}, \quad (2)$$

$$\frac{dB_N}{dt} = s - k_1\overline{R_{bound}}B_N - d_1B_N, \quad (3)$$

$$\frac{dB_0}{dt} = \theta(k_1\overline{R_{bound}}B_N - k_2B_0) - (1-\theta)(d_3B_0), \quad (4)$$

$$\frac{dB_1}{dt} = \theta(k_2B_0 - k_3B_1) - (1-\theta)(d_3B_1), \quad (5)$$

$$\frac{dB_i}{dt} = \theta(ck_3B_{i-1} - k_3B_i) - (1-\theta)(d_3B_i) \quad (i = 2\ldots10), \quad (6)$$

$$\frac{dB_P}{dt} = \theta(ck_3B_{10}) - d_2B_P, \quad (7)$$

Table 1
Variables used in the immune suppression model

Variables	Description
S_{blood}	SRBCs in blood
S_{spleen}	SRBCs trapped in spleen
B_N	Naïve B-cells responding to SRBCs
B_0	Naïve B-cells stimulated by SRBCs before initiation of division
B_i	Dividing B-cells; i denotes the stage of division
B_P	Antibody secreting plasma cells
Ab^I	Anti-SRBC antibody produced from plasma cells
Ab^E	Administered intact anti-SRBC antibody
F_{ab}	Administered anti-SRBC $F(ab')_2$ fragment

$$\frac{dAb^I}{dt} = k_4B_P - d_4(Ab^I - IC^I) - \rho_{liver}S_{blood}\overline{IC^I} - \delta S_{spleen}\overline{IC^I}, \quad (8)$$

$$\frac{dAb^E}{dt} = -d_4(Ab^E - IC^E) - \rho_{liver}S_{blood}\overline{IC^E} - \delta S_{spleen}\overline{IC^E}, \quad (9)$$

$$\frac{dF_{ab}}{dt} = -d_5(F_{ab} - IC^{F_{ab}}) - \rho_{liver}S_{blood}\overline{IC^{F_{ab}}} - \delta S_{spleen}\overline{IC^{F_{ab}}}. \quad (10)$$

3.2. Antigen sequestration and clearance

3.2.1. Antigen sequestration from blood to liver and spleen

Eq. (1)

$$\frac{dS_{blood}}{dt} = -\rho_{liver}S_{blood} - \rho_{spleen}S_{blood}$$

has the general structure of

$$\frac{dS_{blood}}{dt} = -\text{Sequestration rate into liver} - \text{Sequestration rate into spleen}.$$

SRBCs injected into mouse blood are sequestered mainly in the liver and spleen. The functions of SRBCs captured by macrophages in the liver (ρ_{liver}) and the spleen (ρ_{spleen}) are dependent on the number of antibodies bound ($\overline{Ab_{bound}}$) to the antigen. $\overline{Ab_{bound}} = \overline{IC^I} + \overline{IC^E}$ denotes the sum of bound antibodies including antibodies secreted by plasma cells and the administered antibodies, but $F(ab')_2$ fragments are not included because they do not mediate phagocytosis. In the term $\overline{Ab_{bound}} = \overline{IC^I} + \overline{IC^E}$, $\overline{IC^I}$ denotes the epitope-secreted antibody complexes per SRBC, and $\overline{IC^E}$ denotes the epitope-administered antibody complexes per SRBC (see Appendix A). The antibody-dependent ability of the macrophage to trap antigen is obtained with the Hill function, wherein the sigmoid curve

Table 2
Parameters used in the model

Parameter	Description	Value	Range	Unit	Ref.
s	Naïve B-cell production from bone marrow	6		B-cell/day	
k_1	B-cell stimulation	1.8×10^{-3}		1/(BCR-epitope × day)	
k_2	Delay of stimulated B-cell for division	1		1/day	(Hodgkin et al., 1996)
k_3	B-cell division	3	[3–4]	1/day	(Hodgkin et al., 1996)
k_4	Antibody production from plasma cell	10^8	$[1 \times 10^8–1 \times 10^9]$	Ab/day	(Bachmann et al., 1994; Bocharov and Romanyukha, 1994; Leanderson et al., 1992)
d_1	Naïve B-cell death	0.1	[0.1–0.17]	1/day	(Fulcher and Basten, 1997)
d_2	Plasma cell death	0.4	[0.23–0.5]	1/day	(Bocharov and Romanyukha, 1994; Funk et al., 1998; Rundell et al., 1998)
d_3	Arrest of proliferating B-cell in absence of antigen	0.35		1/day	(Pittner and Snow, 1998)
d_4	Antibody degradation	0.18	[0.17–0.19]	1/day	(Junghans and Anderson, 1996)
d_5	$F(ab)_2$ degradation	0.36		1/day	(Cerottini et al., 1969; Heyman, 1990)
c	Produced daughter cells through division	2			

Table 3
Variable-dependent parameters

Parameter	Description
$PFC = \sum_{i=0}^{10} B_i + B_P$	Total number of activated B cells
$B^* = B_N + \sum_{i=0}^{10} B_i$	Total number of BCR-containing B-cells
$R_T = eB^*$	Total number of BCRs in the B-cell population that can recognize epitopes on SRBCs
$\overline{R_{bound}} = \frac{R_T}{Ab^I + R_T} C_1 \frac{1}{B^*}$	Number of epitope-bound BCRs per B-cell[a]
$\theta = \begin{cases} 1 & \text{for } \overline{R_{bound}} \geqslant \overline{R_\theta} \\ 0 & \text{for } \overline{R_{bound}} < \overline{R_\theta} \end{cases}$	If survival signal is sufficient, $\theta = 1$; otherwise $\theta = 0$
$IC^I = \frac{Ab^I}{Ab^I + R_T} C_1$	Total number of epitope-plasma cell-produced antibody complexes[a]
$IC^E = \frac{Ab^E}{Ab^E + F_{ab}} C_2$ [a]	Total number of epitope-administered antibody complexes[a]
$IC^{F_{ab}} = \frac{F_{ab}}{Ab^E + F_{ab}} C_2$	Total number of epitope-$F(ab)_2$ complexes[a]
$\overline{IC^I} = \frac{IC^I}{S_{blood} + S_{spleen}}$	Number of epitopes covered by plasma cell-produced antibodies per SRBC
$\overline{IC^E} = \frac{IC^E}{S_{blood} + S_{spleen}}$	Number of epitopes covered by administered antibodies per SRBC
$\overline{IC^{F_{ab}}} = \frac{IC^{F_{ab}}}{S_{blood} + S_{spleen}}$	Number of epitopes covered by $F(ab)_2$ fragments per SRBC
$\overline{Ab_{bound}} = \overline{IC^I} + \overline{IC^E}$	Bound antibodies per SRBC ($\overline{Ab_{bound}} = \overline{IC^I} + \overline{IC^E}$) that are able to mediate phagocytosis.
$\rho_{liver} = (\omega_{liver}^{ops} - \omega_{liver}^{non}) \frac{\left[\overline{Ab_{bound}}\right]^{n_{trap}}}{\left[\overline{Ab_{bound}}\right]^{n_{trap}} + H_{trap}^{n_{trap}}} + \omega_{liver}^{non}$	Bound antibody-dependent rate of SRBC sequestration in liver
$\rho_{spleen} = (\omega_{spleen}^{ops} - \omega_{spleen}^{non}) \frac{\left[\overline{Ab_{bound}}\right]^{n_{trap}}}{\left[\overline{Ab_{bound}}\right]^{n_{trap}} + H_{trap}^{n_{trap}}} + \omega_{spleen}^{non}$	Bound antibody-dependent rate of SRBC sequestration in spleen
$\delta = \rho_{spleen} \frac{4.11 + 282.6 \times \left[\overline{Ab_{bound}}\right]^{0.9} / \left[\overline{Ab_{bound}}\right]^{0.9} + 11710.3^{0.9}}{155.0 + 1317 \times \left[\overline{Ab_{bound}}\right]^{2.19} / \left[\overline{Ab_{bound}}\right]^{2.19} + 4088.8^{2.19}}$	Bound antibody-dependent rate of SRBC phagocytosis in spleen

[a]In the equations, C_1 denotes the sum of epitope-plasma cell-produced antibody complexes and epitope-BCR complexes, and C_2 denotes the sum of epitope-administered antibody complexes and epitope-$F(ab')_2$ fragment complexes (see Appendix A).

Table 4
Values used for the variable-dependent parameters

Parameter	Description	Value	Range	Unit	Ref.
g	Number of epitopes per SRBC	106	[10^6–?]		(Kumpel, 2002; Kumpel and Elson, 2001)
b	Number of BCRs per B-cell	105			(Agrawal and Linderman, 1996)
e_0	Total number of epitopes on 2×10^4 SRBCs	2×10^{11}			
B_N^0	Number of naïve B-cells at steady state	60	[48–66]		(Kettman and Dutton, 1970; Möller and Wigzell, 1965)
$R_0 = bB_N^0$	Total number of BCRs on 60 B-cells at steady state	6×10^6			
$\overline{R_{act}}$	Minimum number of BCR-epitope complexes for B-cell stimulation	111			
$\overline{R_0}$	Minimum number of BCR-epitope complexes for B-cell survival	666			(Donahue and Fruman, 2003)
K_A^I	Affinity of BCR and produced Ab to epitope	5.55×10^{-14}		IC/(epitope × Ab)	
K_A^E	Affinity of administered Ab or F(ab′)$_2$ fragments to epitope		[5.55×10^{-16}–5.55×10^{-12}]	IC/(epitope × Ab)	
ω_{liver}^{ops}	Rate constant for sequestration of antibody-coated SRBCs in liver	6.65		1/day	(Bezdicek et al., 1999)
ω_{liver}^{non}	Rate constant for sequestration of SRBCs in liver	3.26		1/day	(Bezdicek et al., 1999; Guo et al., 2000)
ω_{spleen}^{ops}	Rate constant for sequestration of antibody-coated SRBCs in spleen.	6.65		1/day	(Bezdicek et al., 1999)
ω_{spleen}^{non}	Rate constant for sequestration of SRBCs in spleen.	1.63	[0.54–3.26]	1/day	(Bezdicek et al., 1999; Guo et al., 2000)
n_{trap}	Coefficient of the Hill function for SRBC trapping	2.19			(Miklós et al., 1993)
H_{trap}	Coefficient of the Hill function for SRBC trapping	4088.8			(Miklós et al., 1993)
n_{ingest}	Coefficient of the Hill function for SRBC ingestion	0.9			(Miklós et al., 1993)
H_{ingest}	Coefficient of the Hill function for SRBC ingestion	11710.3			(Miklós et al., 1993)

effectively represents the experimental results of antibody-dependent saturation described by Miklós et al. (1993) (Fig. 2). The ρ_{liver} and ρ_{spleen} values at $\overline{Ab_{bound}} = 0$ represent the natural ability to trap macrophages without the aid of the antibody, which occurs at the beginning of the immune response. The antibody-mediated capture of SRBCs is saturated because more than 10,000 antibodies are bound to each SRBC ($\overline{Ab_{bound}} > 10,000$) (Fig. 2A) (Miklós et al., 1993).

Eqs. (11) and (12) were obtained by fitting the Hill function ($A + B\times\overline{Ab_{bound}}^n \big/ \overline{Ab_{bound}}^n + H^n$) to the experimental data in Fig. 2A and B, respectively (Miklós et al., 1993). Ω_{bound} and $\Omega_{ingested}$ respectively denote the number of SRBCs bound to macrophages and the number of SRBCs ingested by macrophages according to the number of bound antibodies per SRBC.

$$\Omega_{bound} = 155.0 + 1317\times\frac{\left[\overline{Ab_{bound}}\right]^{2.19}}{\left[\overline{Ab_{bound}}\right]^{2.19} + 4088.8^{2.19}}, \quad (11)$$

$$\Omega_{ingested} = 4.11 + 282.6\times\frac{\left[\overline{Ab_{bound}}\right]^{0.9}}{\left[\overline{Ab_{bound}}\right]^{0.9} + 11710.3^{0.9}}. \quad (12)$$

However, the results in Fig. 2 were obtained from in vitro experiments with 100 macrophages cultured in a small volume. If real physiological conditions were considered, although the relationships might differ from the estimated equations, they would be still proportional to the satura-

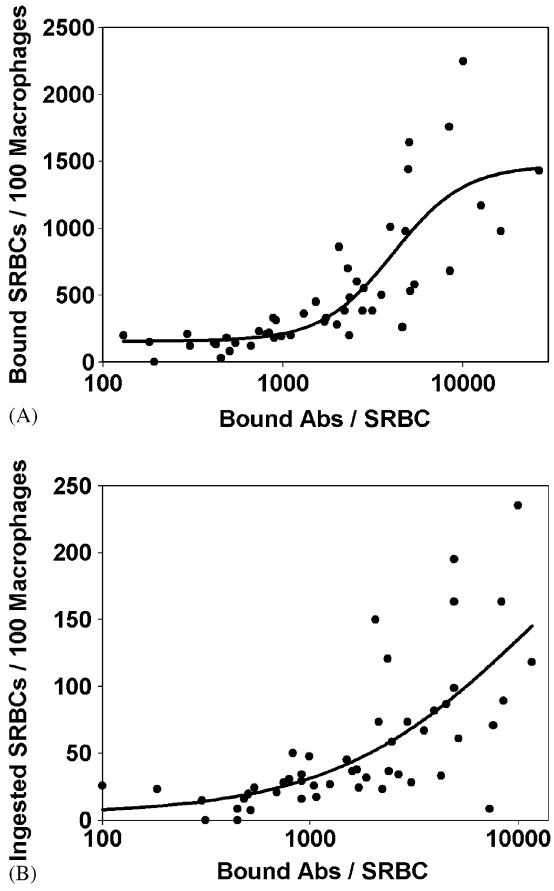

Fig. 2. Relationship between the number of bound antibodies and macrophage activities. Experimental data for macrophage trapping (A) and ingestion (B) of SRBCs were obtained from Miklós et al. (1993). Because the number of trapped or ingested SRBCs is saturated in excess of bound antibodies, the data were fitted to an S-shaped curve with a Hill function: $(\max - \min)[\text{Bound Ab}]^n/([\text{Bound Ab}]^n + H^n) + \min$. The estimated parameters were $n = 2.19$ and $H = 4088.8$ for SRBC trapping and $n = 0.9$ and $H = 11710.3$ for SRBC ingestion. Ab, antibody.

tion curve for bound antibody $\overline{Ab_{bound}}^n/(\overline{Ab_{bound}}^n + H^n)$, which is captured by function (13). The expressions 'max rate' and 'min rate' denote the trapping rate of antibody-coated and non-coated SRBCs, respectively. The trapping rate in the liver and spleen are specified by Eqs. (14) and (15). ω_{liver}^{ops} denotes the trapping rate of fully coated SRBCs by the liver, ω_{liver}^{non} the trapping rate of non-coated SRBCs by the liver, ω_{spleen}^{ops} the trapping rate of fully coated SRBCs by the spleen, and ω_{spleen}^{non} the trapping rate of non-coated SRBCs by the spleen. Finally, *ops* represents "opsonized" (fully coated by antibodies) antigen and *non* represents "non-opsonized" antigen.

$$\rho = ([\text{max rate}] - [\text{min rate}])\frac{[\text{bound Ab}]^n}{[\text{bound Ab}]^n + H^n} + [\text{min rate}], \tag{13}$$

$$\rho_{liver} = (\omega_{liver}^{ops} - \omega_{liver}^{non})\frac{\left[\overline{Ab_{bound}}\right]^{n_{trap}}}{\left[\overline{Ab_{bound}}\right]^{n_{trap}} + H_{trap}^{n_{trap}}} + \omega_{liver}^{non}, \tag{14}$$

$$\rho_{spleen} = (\omega_{spleen}^{ops} - \omega_{spleen}^{non})\frac{\left[\overline{Ab_{bound}}\right]^{n_{trap}}}{\left[\overline{Ab_{bound}}\right]^{n_{trap}} + H_{trap}^{n_{trap}}} + \omega_{spleen}^{non}. \tag{15}$$

There are three times more antigen-trapping macrophages in the liver than in the spleen (Lee et al., 1985), and 2–6 times more SRBCs are trapped in the liver (Guo et al., 2000; Ouchi et al., 1976; van Rijen et al., 1998). Thus, before immunization, SRBCs are rapidly cleared from blood and ~80% of them are sequestered in the liver (Guo et al., 2000; Rihova and Vetvicka, 1984; van Rijen et al., 1998). The clearance rate of antibody-coated antigens is proportional to the number of bound antibodies (Miklós et al., 1992, 1993). Thus, antibody-coated SRBCs are much more rapidly trapped and phagocytosed by macrophages, with an estimated half-life ($t_{1/2}$) of 75 min in the blood (Bezdicek et al., 1999). Because antibody-coated antigens are sequestered equally in the liver and spleen, the trapping rates of antibody-coated SRBCs in each organ are approximately 6.65 days (Bezdicek et al., 1999). The trapping rates for uncoated SRBCs are reduced by $\frac{1}{2}$ in the liver and $\frac{1}{2}$–$\frac{1}{6}$ in the spleen compared to antibody-coated SRBCs (Bezdicek et al., 1999; Guo et al., 2000). Therefore, the trapping rate of antibody-coated SRBCs is 3.26 and 1.63 days^{-1} in liver and spleen, respectively.

3.2.2. Antigen clearance in the spleen

Because trapped antigens in the spleen are a major source of the immune response and degradation in liver is a natural process for eliminating senescent RBCs (Mohr et al., 1987; Naito et al., 1997), only phagocytosis in the spleen was considered.

Eq. (2)

$$\frac{dS_{spleen}}{dt} = \rho_{spleen}S_{blood} - \delta S_{spleen}$$

has the general structure of

$$\frac{dS_{spleen}}{dt} = \text{Sequesteration rate into spleen} - \text{Removal rate by macrophages.}$$

3.2.2.1. Sequestration rate into spleen. SRBCs injected into the blood are captured by macrophages in the spleen. The rate of capture is proportional to the bound antibody/SRBC-dependent parameter, ρ_{spleen}.

3.2.2.2. Removal rate by macrophages. The phagocytosis rate parameter δ was estimated by Eq. (16), which assumes that the ratio of the in vivo phagocytosis rate to the capture rate is proportional to the ratio of the in vitro rates.

$$\delta = \rho_{spleen}\frac{\Omega_{ingested}}{\Omega_{bound}}. \tag{16}$$

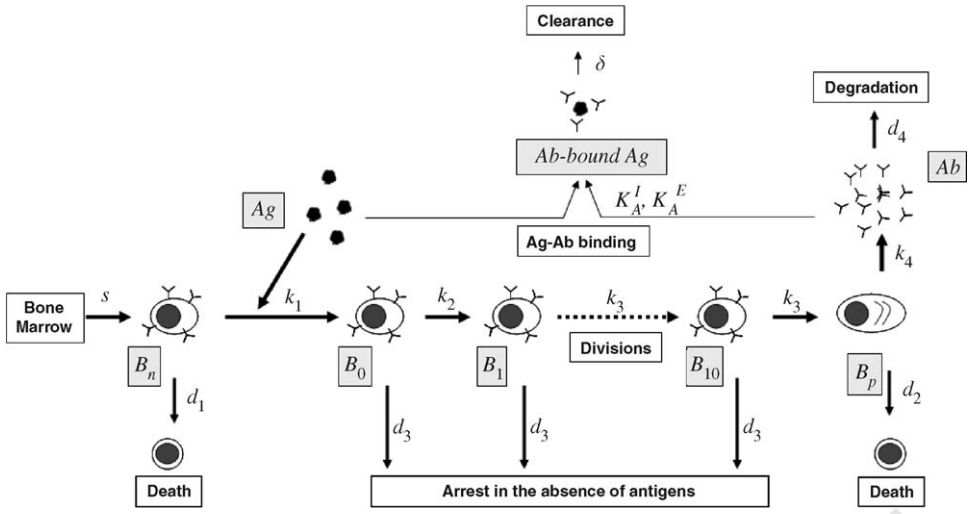

Fig. 3. Humoral immune response in the model. In spleen, B-cells are stimulated by antigens (Ag). The stimulated B-cells proliferate only after a 1-day delay. They differentiate into antibody (Ab)-secreting plasma cells, but, in the absence of antigens, death of the stimulated B-cells is induced. The secreted antibodies bind to epitopes on antigens and mediate rapid clearance, for example, via macrophages.

3.3. B-cell proliferation

If enough epitopes are recognized via BCRs, they trigger activation of the B cell. After a 1-day delay, the activated B cells divide on average 10 times (Andersson et al., 1977; Hodgkin et al., 1996; Melchers and Andersson, 1986). Unlike the B-cell activation process, wherein BCR-epitope complexes trigger activation signaling, the complexes trigger survival signaling during the proliferation period (Rosado and Freitas, 1998; Smith and Reth, 2004). In other words, B-cell death is induced in the absence of sufficient BCR-epitope complexes (Pittner and Snow, 1998).

Plasma cells produce anti-SRBC antibodies. These antibodies, in turn, bind to epitopes on the SRBCs to mediate phagocytosis via phagocytotic cells, a process that occurs at a rate proportional to the number of bound antibody molecules per SRBC (Miklós et al., 1992, 1993; Tolnay et al., 1992a). The overall B-cell process is depicted in Fig. 3.

3.3.1. B-cell stimulation

Eq. (3)

$$\frac{dB_N}{dt} = s - k_1\overline{R_{bound}}B_N - d_1B_N$$

has the general structure of

$$\frac{dB_N}{dt} = \text{Production rate} - \text{Stimulation rate} - \text{Death rate}.$$

3.3.1.1. B-cell production and death rates. When SRBCs are administered to mice, about 60 naïve B cells recognize the antigens. The antigen-activated B cells then proliferate and differentiate into plasma cells (Kettman and Dutton, 1970; Möller and Wigzell, 1965). The death rate constant for naïve B cells (d_1) is 0.1 days^{-1} (Fulcher and Basten, 1997). We therefore adjusted the production rate of naïve B cells from bone marrow to sustain the number of naïve B cell at a normal level ($s = 6$).

3.3.1.2. Stimulation rate. The stimulation rate constant (k_1) for naïve B cells by SRBCs is inversely proportional to the time required for B-cell activation (< 1 day; t_{act}) and to the number of SRBCs necessary to induce B-cell activation (10^5 SRBCs), but actually 20% of the 10^5 SRBCs are captured in the spleen for the B-cell activation (2×10^4; Ag_{act}) (Guo et al., 2000; Kettman and Dutton, 1970; Möller and Wigzell, 1965; Ouchi et al., 1976; van Rijen et al., 1998). Thus, the B-cell activation rate constant is $1/t_{act}Ag_{act}$. However, to address the relationship between epitope masking and immune suppression using the model, epitopes, not antigens, should be considered. For this purpose, instead of the antigen number, the number of BCR-epitope complexes per B cell needed for activation should be used; $k_1 = 1/(t_{act}\overline{R_{act}})$.

SRBCs have approximately 10^6 epitopes per cell. For initiation of a humoral immune response, 2×10^4 SRBCs, corresponding to 2×10^{10} (e_0) free epitopes, are required (Kumpel, 2002; Kumpel and Elson, 2001). After injecting the antigens, 60 naïve B cells (B_N^0), containing 6×10^6 BCRs (R_0), can recognize the epitopes because each B cell has 10^5 BCRs on its membrane (Agrawal and Linderman, 1996). The number of BCR-epitope complexes per B cell required for activation ($\overline{R_{act}}$) can be estimated by equilibrium kinetics (see Appendix B for a detail description) as described in function (17) where e_0 denotes the number of epitopes on 2×10^4 SRBCs, R_0 is the number of BCRs on 60 B cells, K_A^I is the affinity of plasma cell-produced antibody, and B_N^0 is the number of naïve B cells at the steady state. The experimentally determined affinity of

anti-SRBC antibodies ranges from ~10^7 to $10^9\,\mathrm{nM}^{-1}$, which is much higher than that of the human anti-D polyclonal antibody ($3\times10^8\,\mathrm{M}^{-1}$) and rabbit anti-Hg polyclonal antibody ($10^8\,\mathrm{M}^{-1}$) (Kumpel and Elson, 2001). The anti-SRBC antibodies probably have an unusually high affinity because they were obtained from hyperimmunized mice (Heyman and Wigzell, 1984). Because the humoral immune response in our model is a primary response, we instead used the common polyclonal antibody affinity from human or rabbit ($10^8\,\mathrm{M}^{-1}$) (Kumpel and Elson, 2001). Furthermore, because the structure of the epitope-recognition part of the BCR is the same as that of secreted antibodies, we used the same antibody affinity for the BCR affinity. For consistency in the units, we converted the affinity to 5.55×10^{-14} IC/(epitope × Ab) (K_A^I). Using the mouse mean blood volume (3 ml), we calculated that 111 BCR-epitope complexes are required for activation of one naïve B cell ($\overline{R_{act}}=111$); thus, the B-cell activation rate constant is $k_1=1/(t_{act}\overline{R_{act}})$

$$\overline{R_{act}}=\frac{e_0+R_0+1/K_A^I-\sqrt{(e_0+R_0+1/K_A^I)^2-4e_0R_0}}{2}\frac{1}{B_N^0}. \tag{17}$$

3.3.2. B-cell delay

Eq. (4)

$$\frac{\mathrm{d}B_0}{\mathrm{d}t}=\theta(k_1\overline{R_{bound}}B_N-k_2B_0)-(1-\theta)(d_3B_0)$$

has the general structure of

$$\frac{\mathrm{d}B_0}{\mathrm{d}t}=\theta(\text{Stimulation rate}-\text{Delay rate})-(1-\theta)\,\text{Apoptosis rate},$$

$$\text{where }\theta=\begin{cases}1 & \text{for } \overline{R_{bound}}\geqslant\overline{R_\theta}\\ 0 & \text{for } \overline{R_{bound}}<\overline{R_\theta}\end{cases}.$$

$\overline{R_{bound}}$ denotes the number of BCR-epitope complexes per B cell, and $\overline{R_\theta}$ denotes the minimum number of BCR-epitope complexes per B cell for a B cell to survive and to continue dividing. The function θ determines whether the cell proliferates or dies. In the presence of sufficient BCR-epitope complexes, $\theta=1$; otherwise, $(1-\theta)=0$. For $\theta=1$, the stimulation and delay rates are applied to the differential equation, while the apoptosis rate is ignored and vice versa. For successive divisions, about six-fold more antigenic signal is required than for B-cell activation; hence, $\overline{R_\theta}=6\times\overline{R_{act}}$ (Donahue and Fruman, 2003).

3.3.2.1. Stimulation rate. The stimulated naïve B cells enter the first stage (B_0) of proliferation.

3.3.2.2. Delay rate. Naïve B cells stimulated by antigens start to divide after a 1-day delay (Hodgkin et al., 1996). The rate constant k_1 represents the delay.

3.3.2.3. Apoptosis rate. In the absence of sufficient antigenic signal (BCR-epitope complex), the cell cycle ceases and B-cell apoptosis is induced with a half-life of 2 days, $d_3=0.35$ (Pittner and Snow, 1998).

3.3.3. B-cell proliferation

Eqs. (5) and (6)

$$\frac{\mathrm{d}B_1}{\mathrm{d}t}=\theta(k_2B_0-k_3B_1)-(1-\theta)(d_3B_1),$$

$$\frac{\mathrm{d}B_i}{\mathrm{d}t}=\theta(ck_3B_{i-1}-k_3B_i)-(1-\theta)(d_3B_i)\quad(i=2\ldots10)$$

have the general structures of

$$\frac{\mathrm{d}B_1}{\mathrm{d}t}=\theta(\text{Delay rate}-\text{Division rate})-(1-\theta)\,\text{Apoptosis rate},$$

$$\frac{\mathrm{d}B_i}{\mathrm{d}t}=\theta(\text{B cell production rate}-\text{Division rate})-(1-\theta)\,\text{Apoptosis rate}.$$

On average, activated B cells undergo 10 successive divisions. Therefore, we incorporated 11 stages of proliferation including the delay stage (Andersson et al., 1977; Melchers and Andersson, 1986).

3.3.3.1. Delay rate. After a 1-day delay, stimulated B cells enter the clonal expansion stage in which they start to divide.

3.3.3.2. Division rate. Activated B cells undergo clonal expansion with a constant division rate (6–8 h; $k_3=3$) in the presence of sufficient antigenic signals (Hodgkin et al., 1996; Jhagvaral Hasbold, 1998).

3.3.3.3. B-cell production rate. During each cell division, new B cells enter the next division stage, i. The coefficient c represents the increase in the number of B cells through one division.

3.3.3.4. Apoptosis rate. As explained in Section 3.3.2.3, in the absence of sufficient BCR-epitope complexes, proliferating B cells arrest and undergo cell death with a half-life of 2 days.

3.3.4. Plasma cells

Eq. (7)

$$\frac{\mathrm{d}B_P}{\mathrm{d}t}=\theta(ck_3B_{10})-d_2B_P$$

has the general structure of

$$\frac{\mathrm{d}B_P}{\mathrm{d}t}=\theta\,\text{Differentiation rate}-\text{Death rate}.$$

3.3.4.1. Differentiation rate. After completing divisions, B cells differentiate into antibody-secreting plasma cells.

3.3.4.2. Death rate. The half-life of a plasma cell is 2–3 days (Bocharov and Romanyukha, 1994; Funk et al., 1998; Rundell et al., 1998). Eq. (7) does not include the apoptosis induced by a decreased antigenic signal. Although activated B cells require a survival signal, plasma cells do not seem to require such a signal because, due to the loss of BCRs, they cannot interact with antigens (Calame et al., 2003).

3.4. Antibody reactions

3.4.1. Antibody production

Eq. (8)

$$\frac{dAb^I}{dt} = k_4 B_P - d_4(Ab^I - IC^I) - \rho_{liver} S_{blood} \overline{IC^I} - \delta S_{Spleen} \overline{IC^I}$$

has the general structure of

$$\frac{dAb^I}{dt} = \text{Production rate} - \text{Decay rate of unbound Ab} - \text{Removal rate of SRBC-bound Ab in liver} - \text{Removal rate of SRBC-bound Ab via phagocytosis in spleen.}$$

3.4.1.1. Production rate. Plasma cells produce 10^8–10^9 antibodies per day (Bachmann et al., 1994; Leanderson et al., 1992). The parameter $k_4 = 10^8$ Ab/day represents the number of antibodies produced from a plasma cell per day.

3.4.1.2. Decay rate of unbound antibody. Unbound antibodies are degraded at the rate of $d_4 = 0.18$/day. In the term $d_4(Ab^I - IC^I)$, Ab^I denotes produced antibodies and IC^I denotes epitope-antibody complexes so that $(Ab^I - IC^I)$ represents "unbound plasma cell-produced antibodies".

3.4.1.3. Removal rate of SRBC-bound antibodies in the liver. Secreted antibodies bind to epitopes and mediate SRBC phagocytosis at a rate proportional to the number of bound antibodies (Miklós et al., 1992, 1993; Tolnay et al., 1992a). SRBCs injected into the blood are captured by macrophages and eliminated via phagocytosis in the liver and spleen. During phagocytosis of SRBCs, the bound antibodies are also eliminated. Because SRBCs sequestered in liver do not induce an immune response, the sequestration of SRBCs in the liver actually represents their elimination. In the term $\rho_{liver} S_{blood} \overline{IC^I}$, $\rho_{liver} S_{blood}$ is the rate of SRBC sequestration from the blood by the liver so that the coelimination of the bound antibodies is proportional to the rate of SRBC elimination and to the number of bound antibodies. The parameter ρ_{liver} represents the rate of antibody-dependent sequestration. $\overline{IC^I}$ denotes the number of epitope and plasma cell produced-antibody complexes per SRBC (see Appendix A for $\overline{Ab_{bound}}$ and $\overline{IC^I}$).

3.4.1.4. Removal rate of SRBC-bound antibodies via phagocytosis in the spleen. Sequestered SRBCs are eliminated by macrophages via phagocytosis in the spleen. The term $\delta S_{Spleen} \overline{IC^I}$ represents the co-elimination of bound antibodies with the sequestered SRBCs by macrophages in the spleen, and δ represents the bound antibody-dependent phagocytosis rate.

3.4.2. Administered antibodies

Eq. (9)

$$\frac{dAb^E}{dt} = -d_4(Ab^E - IC^E) - \rho_{liver} S_{blood} \overline{IC^E} - \delta S_{Spleen} \overline{IC^E}.$$

has the general structure of

$$\frac{dAb^E}{dt} = -\text{Decay rate of unbound Ab} - \text{Removal rate of SRBC-bound Ab in liver} - \text{Removal rate of SRBC-bound Ab } \textit{via} \text{ phagocytosis in spleen.}$$

3.4.2.1. Decay rate of unbound antibody. Administered antibody has the same half-life as the antibody produced during the immune response. The term $(Ab^E - IC^E)$ represents the amount of unbound administered antibody.

3.4.2.2. Removal rate of SRBC-bound antibodies in the liver. $\overline{IC^E}$ denotes the number of bound administered antibodies per SRBC. The term $\rho_{liver} S_{blood}$ represents the rate of SRBC removal from the blood by the liver. Thus, the rate of removal of bound antibodies is proportional to the rate of SRBC removal and to the number of bound antibodies.

3.4.2.3. Removal rate of SRBC-bound antibodies via phagocytosis in the spleen. $\overline{IC^E}$ denotes the number of complexes of epitope and administered antibody per SRBC. The antibodies in the complexes are removed by macrophages along with the SRBCs. The removal rate is dependent on the rate of phagocytosis in the spleen, δS_{Spleen}, and the number of administered antibodies bound per SRBC, $\overline{IC^E}$.

3.4.3. Administered $F(ab')_2$ fragments

Eq. (10)

$$\frac{dF_{ab}}{dt} = -d_5(F_{ab} - IC^{F_{ab}}) - \rho_{liver} S_{blood} \overline{IC^{F_{ab}}} - \delta S_{spleen} \overline{IC^{F_{ab}}}$$

has the general structure of

$$\frac{dF_{ab}}{dt} = -\text{Decay rate of unbound Ab} - \text{Removal rate of SRBC-bound } F_{ab} \text{ in liver} - \text{Removal rate of SRBC-bound } F_{ab} \textit{ via} \text{ phagocytosis in spleen.}$$

Administered or plasma cell-produced antibody and $F(ab')_2$ fragment have different half-lives, and $F(ab')_2$ fragments do not mediate phagocytosis. Due to the loss of the Fc portion, the $F(ab')_2$ fragment has a two-fold shorter half-life (d_5) than intact antibodies (Cerottini et al., 1969; Heyman, 1990). Like intact antibodies (produced by plasma cells or administered), $F(ab')_2$ fragments bind to epitopes and are eliminated together with SRBCs by macrophages in the liver and spleen. The term $\rho_{liver} S_{blood} \overline{IC^{F_{ab}}}$ represents the elimination rate of bound $F(ab')_2$ fragments in the liver, and $\delta S_{spleen} \overline{IC^{F_{ab}}}$ represents the removal rate in the spleen. Because they do not mediate phagocytosis, epitope-$F(ab')_2$ complexes were not incorporated into the parameter affecting the rate of phagocytosis, $\overline{Ab_{bound}}$.

4. Results

In the present study, we developed a mathematical model using parameters obtained from the literature or estimated from physiological properties to describe the suppression of the humoral response by the passive administration of antibodies. First, we simulated a normal immune response and compared the results with experimental data reported in the literature. Next, we simulated the effects of antibody affinity, antibody amount, timing of administration, and antibody-mediated phagocytosis on immune suppression. To investigate the contribution of phagocytosis to immune suppression, we modified the model to mimic FcγRI/III knockout mice, which cannot carry out antibody-mediated phagocytosis of SRBCs. Furthermore, instead of intact antibodies, we used $F(ab')_2$ fragments, which have produced conflicting experimental results. The immune suppression simulations were performed using Berkeley Madonna 8.0 with a fourth-order Runge-Kutta method for numerical integration (Cartwright and Piro, 1992).

4.1. Immune response against SRBCs

Using our model, we simulated the immunological response to 4×10^6 SRBCs (Fig. 4). To simulate immunization with SRBCs, the number of SRBCs in the blood at time 0 was set to 4×10^6 ($SRBC_{blood}(0) = 4 \times 10^6$), and all other variables were set to zero. Injected SRBCs were cleared from blood into the liver and spleen within 1 day (Fig. 4A). At day 1, 23% of the injected SRBCs were trapped in the spleen for initiation of an immune response. Three-fold more SRBCs (65%) were trapped in the liver, and 10% remained in the blood. These results are consistent with experimental findings reported by Bezdicek et al. (1999) and Rihova and Vetvicka (1984). Sequestered SRBCs in the spleen were eliminated slowly, but after 2–3 days the removal rate increased due to the increased rate of phagocytosis as a result of antibody production. As shown in Fig. 4B, the number of activated B cells increased starting the first day after immunization and continued for the following 4 days (Möller and Wigzell, 1965), with a peak on day 5 (Enriquez-Rincon and Klaus, 1984). Failure to maintain a sufficient number of BCR-epitope complexes, which acts as a survival signal (Fig. 4C), induced the arrest of proliferating B cells after day 5, causing a decrease in the B-cell population. Production of antibodies resulted in the masking of up to 25% of the epitopes on SRBCs (Fig. 4E). Therefore, according to our simulation, 75% of the epitopes were always available to interact with antibodies or BCRs. This normal immune response is in good agreement with experimental results (Adler, 1965; Henry and Jerne, 1968; Heyman and Wigzell, 1984; Karlsson et al., 1999, 2001a, b).

4.2. Suppression of the humoral immune response by passively administered anti-SRBC antibodies

4.2.1. Effect of the timing of antibody administration on immune suppression

To simulate immune suppression, 10 μg of antibody (4×10^{13} molecules) was administered on days 0, 1, and 2 after immunization (Fig. 5). For the immunization, $SRBC_{blood}$ was set to 4×10^6, and for the antibody administration, the number of antibodies Ab^E was increased by 4×10^{13} at $t = 0$, $t = 1$, or $t = 2$. All other variables were set to zero. The suppression was maximal when antibodies were coadministered with antigens (Fig. 5B). Later administration of antibodies resulted in a weaker suppression of the immune response (Fig. 5B–D) (Möller and Wigzell, 1965). Even in the presence of maximal suppression with a sufficient amount of antibodies (Fig. 5B), there was a measurable immune response because approximately 30% of the epitopes were still free to activate naïve B cells (Fig. 5E) and sustain a survival signal for 1–2 days (Fig. 5F). As shown in Fig. 5B–D and F, the B-cell population markedly decreased 1 day after antibody administration (Möller and Wigzell, 1965) due to B-cell arrest induced by an insufficient survival signal.

4.2.2. Effect of antibody affinity on immune suppression

The humoral response is affected not only by the timing of antibody administration but also by the antibody affinity. To investigate the effect of antibody affinity on immune suppression, anti-SRBC antibodies of different affinities (10^5–$10^8\,M^{-1}$) were administered along with 4×10^6 SRBCs (Fig. 6). A higher affinity antibody was more effective at immune suppression than a lower affinity antibody (Fig. 6A). An antibody with an affinity of $10^8\,M^{-1}$ could mask the majority (~70%) of epitopes, and it successfully suppressed the B-cell population. With low affinity antibodies, the ability to mask epitopes

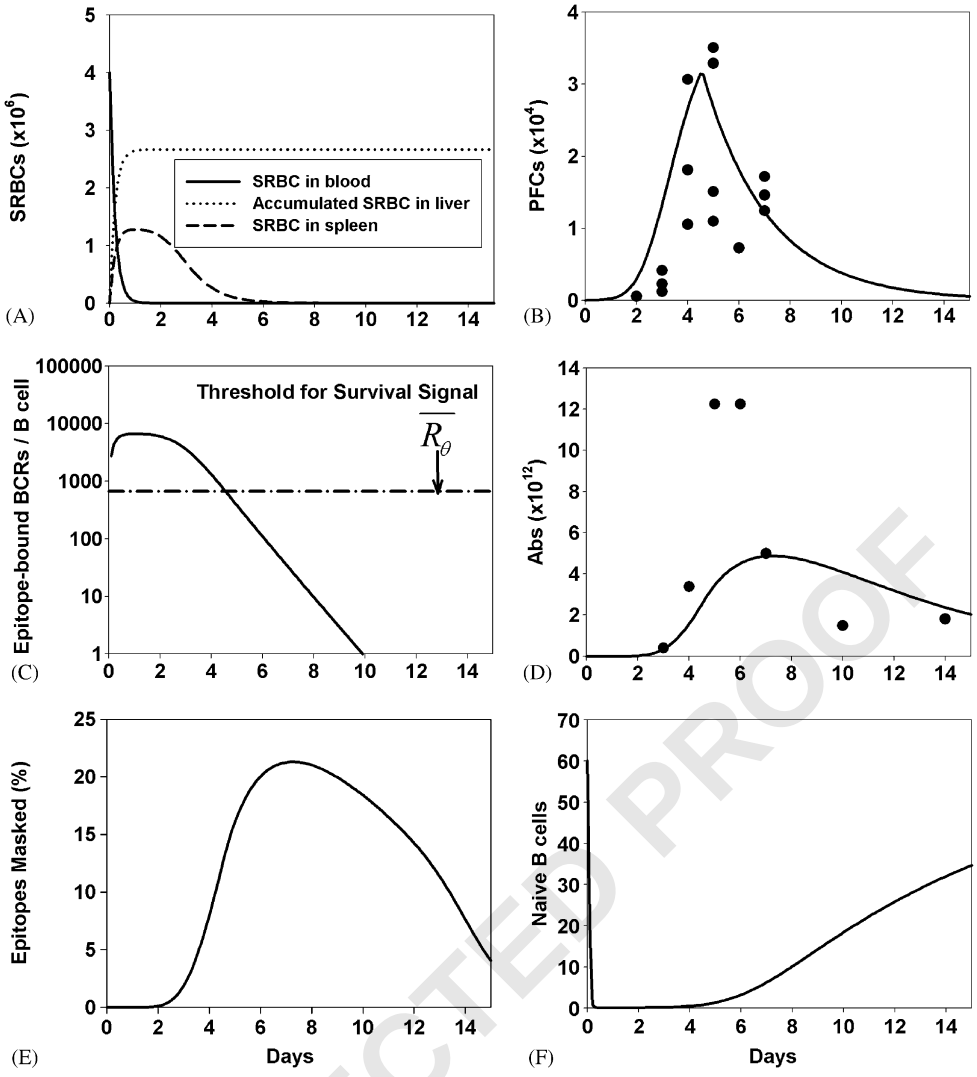

Fig. 4. Immunological profiles against 4×10^6 SRBCs. The model was simulated with injection of 4×10^6 SRBCs. Immunological profiles are shown for number of SRBCs (A), number of activated B-cells (B), number of BCR-epitope complexes per B-cell (C), amount of produced antibody (D), percentage of masked epitopes per SRBC (E), and number of naïve B-cells (F). The percentage of epitopes masked was calculated as $100 \times$ (epitopes masked per SRBC]/[total number of epitopes on a SRBC]. The data points in (B) were obtained from Henry and Jerne (1968), Heyman and Wigzell (1984), and Karlsson et al. (1999, 2001a, b); and those in (D) were from Adler (1965) by assuming that the lowest detectable concentration in the hemolytic test is 10^{-10} M (Henry and Jerne, 1968). SRBCs in the liver shown in (A) was the total number of SRBCs sequestered in liver and is shown for comparison. PFC, plaque forming unit, represents the number of activated B-cells.

dramatically decreased along with their abilities to mediate immune suppression. The increases in the extent of epitope masking 3–4 days after immunization were due to the production of antibodies by plasma cells. An antibody with an affinity of $10^6\,M^{-1}$, however, could also induce significant suppression even though only 2% of the epitopes were masked. This result implies that a mechanism other than epitope masking is central in immune suppression by low-affinity antibodies. As shown in Fig. 6B and D, in spite of the decrease of masked epitopes with time, the number of epitope-BCR complexes also decreased. This was due to repaid elimination of SRBCs, resulting in a decrease in the total number of epitopes (Fig. 6C).

4.2.3. Effect of the amount of antibody on immune suppression

In addition to the timing and affinity, the amount of antibody affects immune suppression (Karlsson et al., 1999). The more antibody administered, the greater the suppression of the immune response (Karlsson et al., 1999; Kumpel, 2002; Kumpel and Elson, 2001). To investigate the relationship between the amount of administered antibody and immune suppression, 0.1–50 μg of antibody with an affinity of $10^8\,M^{-1}$ were administered along with 4×10^6 SRBCs. The initial values were $Ab^E(0) = 1 \times 10^{12} - 2 \times 10^{14}$ and $SRBC_{blood}(0) = 4 \times 10^6$. After the simulations, we calculated the extent of immune response:

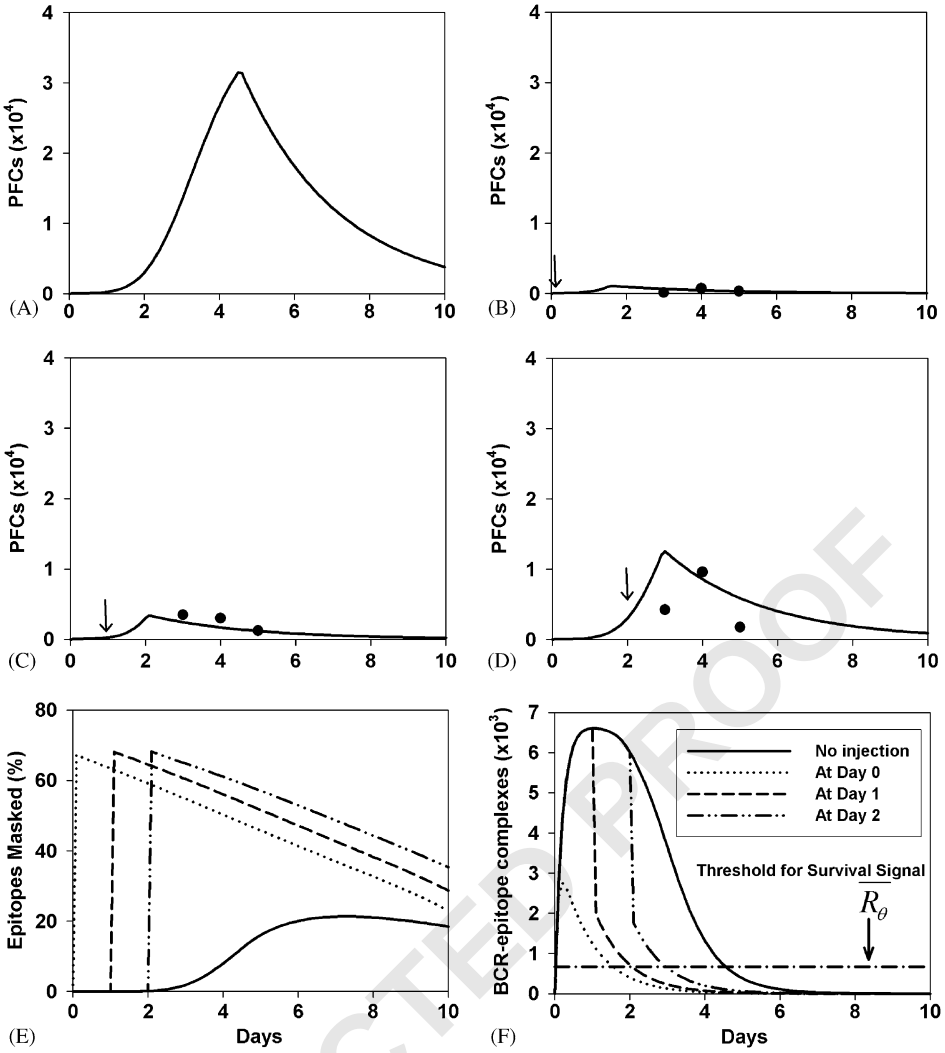

Fig. 5. Effect of the timing of antibody administration on immune suppression. To investigate the effect of the timing of antibody administration on immune suppression, mice were immunized with 4×10^6 SRBCs and administered 10 μg of antibodies on day 0 (B), day 1 (C), or day 2 (D). For comparison, the control response is shown in (A). For detailed investigations, the percentage of epitope masked (E) and the number of BCR-epitope complexes per B-cell (F) are also shown. The legend for graphs (E) and (F) are shown inside graph (F). The minimal signal required for B-cell survival is indicated in (F). The data points in (B)–(D) were obtained from Karlsson et al. (2001b).

% immune response = (Plaque Forming Units (PFC) in antibody injected mice/PFC in control) × 100 (Heyman and Wigzell, 1984). A higher percentage means that the response is less suppressed; for example, 100% means no measurable suppression.

Results of the simulation are shown in Fig. 7. As expected, the more antibodies administered, the more the response was suppressed. For example, 0.1 μg antibody reduced the immune response to 40%, and 50 μg completely suppressed the immune response. Although 50 μg of antibody masked up to 91% of epitopes (Fig. 8) and completely suppressed the B-cell population, 0.1 μg of antibody masked only 1.7% of epitopes but still caused significant immune suppression.

4.3. Simulation of FcγRI/III knockout

To simulate the effects of FcγRI/III knockout, we set the rates of sequestration and phagocytosis for antibody-coated SRBCs to be the same as for uncoated SRBCs to ignore the facilitation of phagocytosis by bound antibodies ($\rho_{liver} = \omega_{liver}^{non}$, $\rho_{spleen} = \omega_{spleen}^{non}$, and $\delta = 0.03$, which were estimated by setting $\overline{Ab_{bound}} = 0$). In the knockout model, 10 μg of antibodies of different affinities were administered along with 4×10^6 SRBCs; the results of the simulation are shown in Fig. 9. Simulation of the mutant showed that the inability of macrophages to clear antigen resulted in a prolonged immune response (Fig. 9A). A low-affinity antibody ($10^6\,M^{-1}$) did not result in significant immune suppression because it could not sufficiently mask epitopes

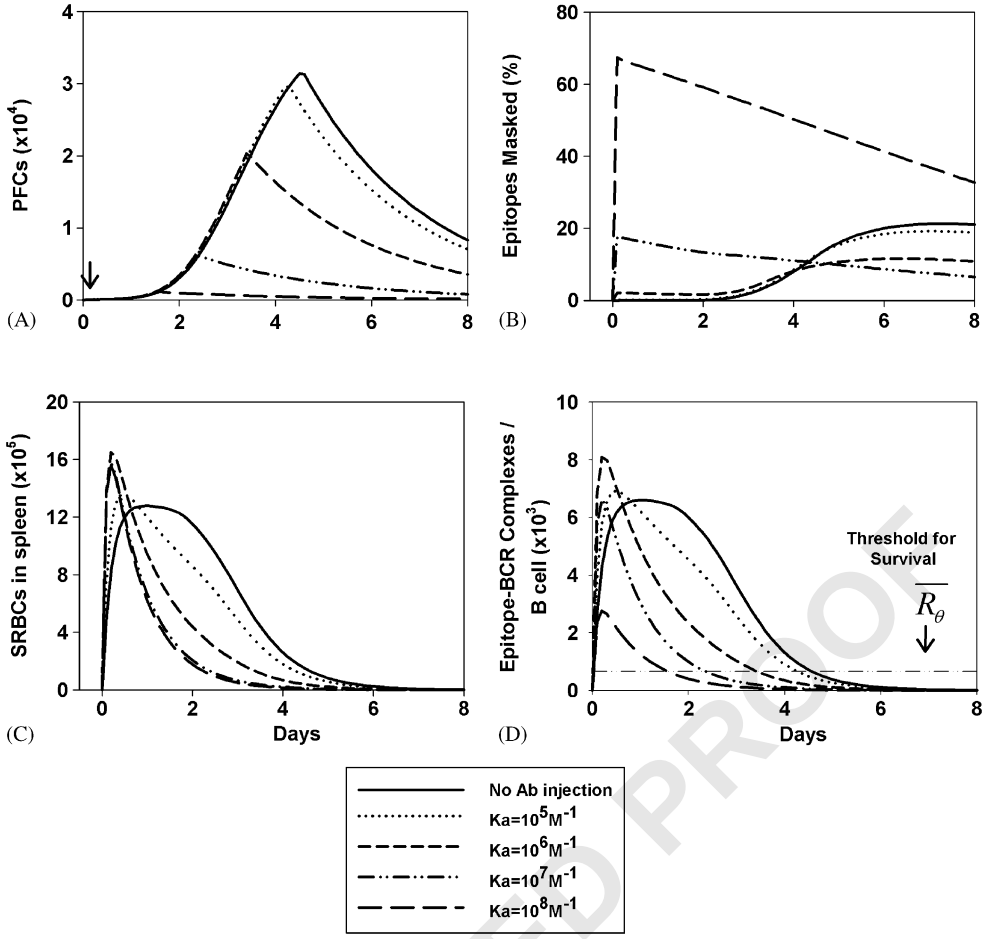

Fig. 6. Effect of the affinity of the administered antibody on immune suppression. For the simulation, 10 μg of antibody with various affinities were coinjected with 4×10^6 SRBCs. The B-cell population (A), percentage of masked epitopes (B), and number of SRBCs in the spleen are shown. There was no significant difference between the control response and that induced by administration of antibody with an affinity of $10^5\,M^{-1}$. A ~$10^6\,M^{-1}$ antibody masked only ~2% of the epitopes, whereas a $10^8\,M^{-1}$ antibody masked up to 70% of the epitopes. The increase of epitope masking after day 3 for the ~$10^6\,M^{-1}$ antibody shown in (B) is due to the production of antibodies by plasma cells.

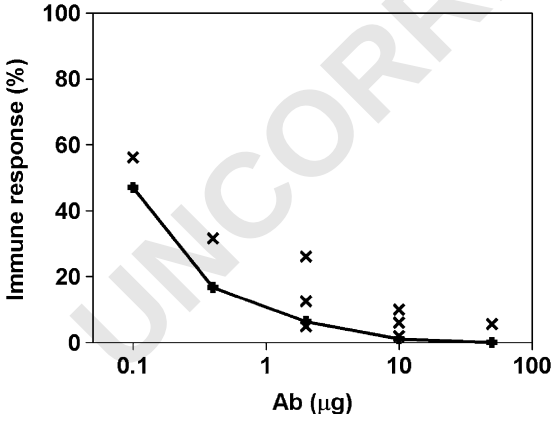

Fig. 7. Effect of the amount of antibody on immune suppression. Between 0.1 and 50 μg of antibodies (Ab) were administered along with 4×10^6 SRBCs, and the percent suppression was calculated on day 5. The percent immune response = 100 × [PFC in antibody injected mice]/[PFC in control]. Data points (x) were obtained from Karlsson et al. (1999, 2001b). The solid line with closed circles represents percentages determined by the simulation. The dashed line represents the response in the control.

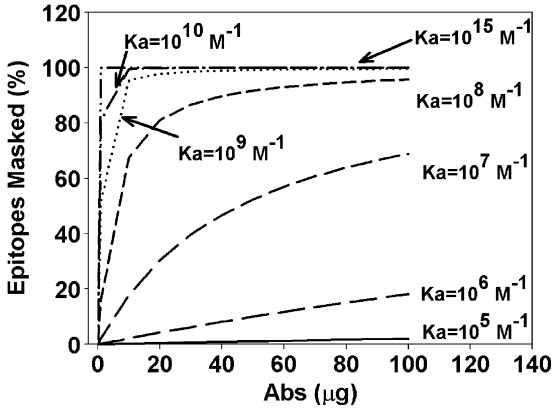

Fig. 8. Effect of the antibody amount and affinity on masking epitopes of 4×10^6 SRBCs. The effects of the antibody (Ab) amount and affinity on epitope masking were investigated. For the $10^5\,M^{-1}$ antibody, even with more than 100 μg of antibody, few epitopes were masked. On the other hand, 10 μg of $10^{10}\,M^{-1}$ antibody could mask all of the epitopes.

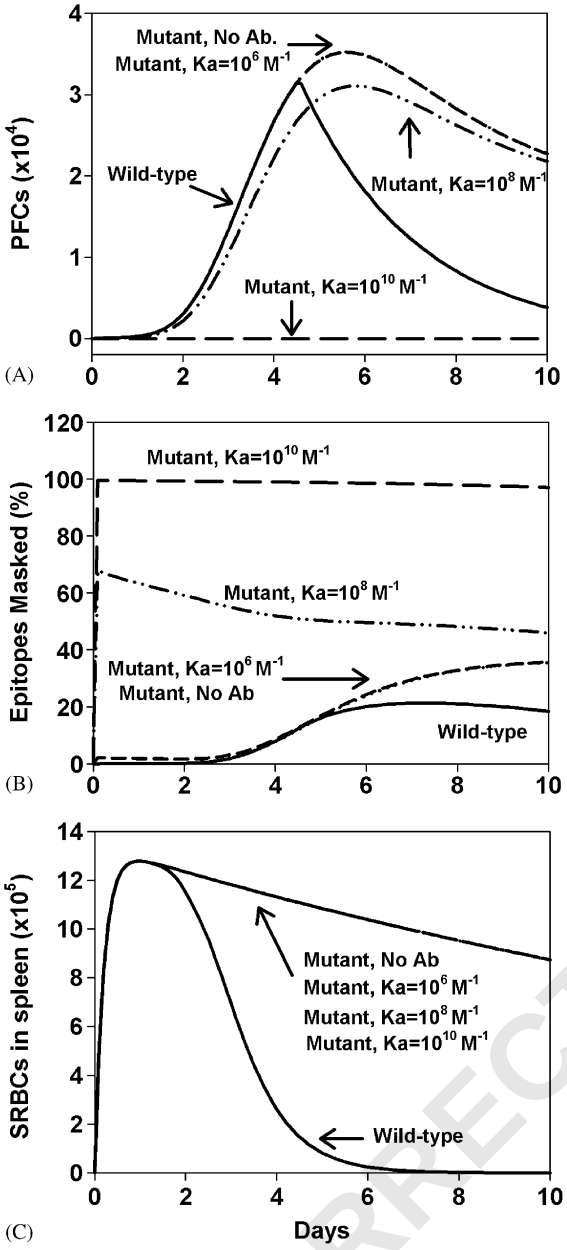

Fig. 9. Simulation of FcγRI+RIII knockout simulation with various antibody affinities. Using a model of the FcγRI+RIII mutant, immune suppression was simulated with antibodies (Ab) with various affinities. A total of 4×10^6 SRBCs with 50 μg of antibody with an affinity of 10^6–$10^{10}\,M^{-1}$ were injected into mutant mice. For comparison, a wild-type model simulation is also shown in each graph. Profiles of B-cell population (A), percentage of masked epitopes (B), and numbers of SRBCs in the spleen (C) are shown. In (C), the SRBC profiles in the mutant and wild-type models were the same.

(Fig. 9A). A higher affinity ($10^8\,M^{-1}$) antibody initially masked ~70% of epitopes, but the remaining 30% of unmasked epitopes were sufficient to activate naïve B cells and deliver an adequate survival signal. Thus, like the $10^6\,M^{-1}$ antibody, the $10^8\,M^{-1}$ antibody did not cause significant suppression. Unlike the low-affinity antibodies, a high-affinity ($10^{10}\,M^{-1}$) antibody covered almost all epitopes, so that it completely inhibited the B-cell response without the aid of macrophages.

4.4. Suppression of the immune response by $F(ab')_2$ fragments

4.4.1. Immune suppression by $F(ab')_2$ fragments with increased half-lives

Experiments with $F(ab')_2$ fragments have produced no suppression, or a similar or 1000-fold weaker suppression compared to intact antibodies (Brüggemann and Rajewsky, 1982; Cerottini et al., 1969; Enriquez-Rincon and Klaus, 1984; Heyman, 1990; Karlsson et al., 1999; Tao and Uhr, 1966). According to the epitope-masking hypothesis, the difference in the Fc-portion of the antibody should not affect immune suppression. Hence, the different results seem to favor FcR-mediated suppression. Researchers that support the epitope masking hypothesis speculate that the lower suppression by $F(ab')_2$ fragments results from a faster rate of decay (Karlsson et al., 1999). We simulated the wild-type model to determine whether the decay rate can explain such different results. For the simulation, we set the following initial values: $SRBC_{blood}(0) = 4\times10^6$ for administration of the fragment; $F_{ab} = 4\times10^{13}$ at $t = 1$; and the $F(ab')_2$ decay rate constant $d_5 = d_4$ to $d_4/4$, where d_4 is the intact antibody decay rate constant. As shown in Fig. 10, although the decay rate was reduced so that of

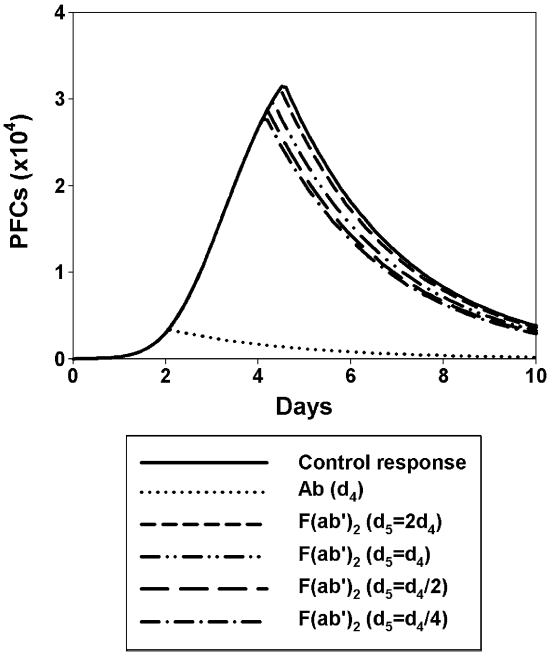

Fig. 10. Comparison of the suppressive abilities of intact Ab, $F(ab')_2$, and $F(ab')_2$ with a prolonged half-life. Fifty μg of antibody (Ab) or $F(ab')_2$ fragments were administered 1 day after immunization with 4×10^6 SRBCs. To investigate the effect of the $F(ab')_2$ degradation rate on immune suppression, the rate constant (d_5) was varied from $d_5 = 2d_4$ to $d_5 = d_4/4$, where d_4 denotes the decay rate constant of intact antibody. In general, $F(ab')_2$'s have a two-fold shorter half-life than intact antibody.

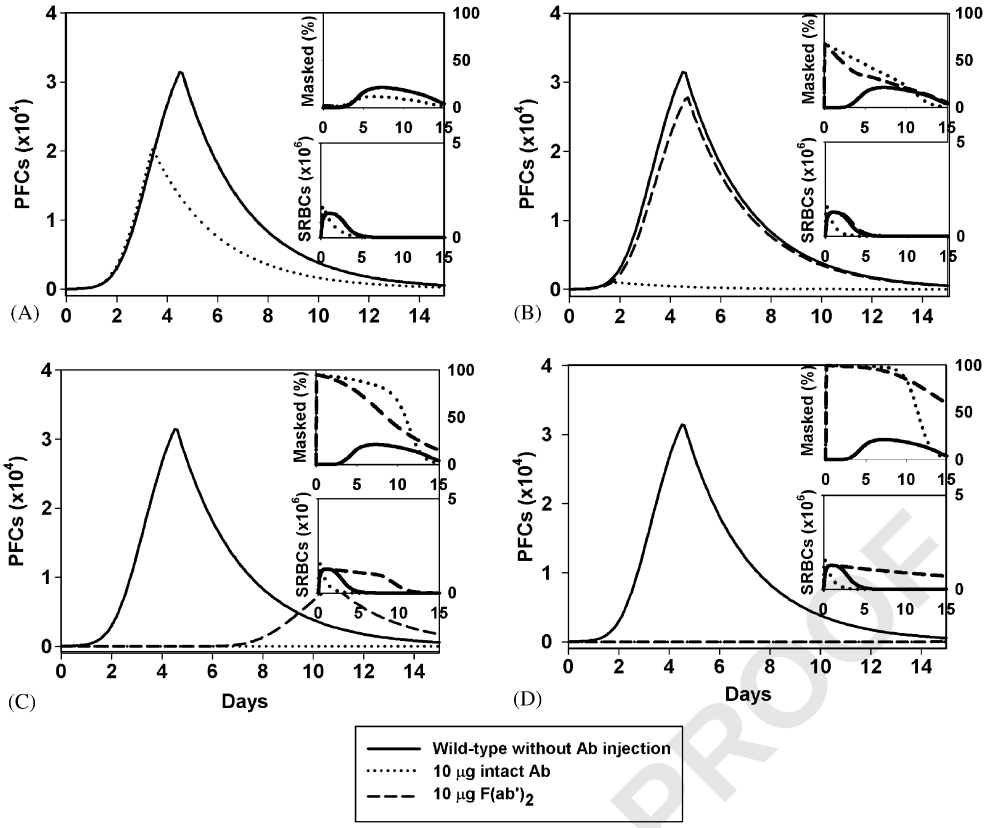

Fig. 11. Immunological profiles by administered $F(ab')_2$ fragments with various affinities. $F(ab')_2$ or intact antibody (Ab) with affinities of $10^6\,M^{-1}$ (A), $10^8\,M^{-1}$ (B), $10^9\,M^{-1}$ (C), or $10^{10}\,M^{-1}$ (D) were administered along with 4×10^6 SRBCs, and their effects on the immune response were determined. In (A), the control response and the response to injection with $F(ab')_2$ overlapped, and in (D) the response to $F(ab')_2$ and intact antibody overlapped. Clearance of SRBCs and masking of epitopes are shown as insets in each graph.

$F(ab')_2$ fragments would remain longer than intact antibodies, the fragments still did not significantly suppress the immune response. Thus, the different results of $F(ab')_2$ and intact antibodies are not the result of different rates of decay.

4.4.2. Suppression of the immune response by $F(ab')_2$ fragments

To further investigate the effect of $F(ab')_2$ on immune suppression, we carried out additional simulations using $F(ab')_2$ with various affinities along with 4×10^6 SRBCs (Fig. 11). For this simulation, $SRBC_{blood}(0)=4\times10^6$, $F_{ab}(0)=4\times10^{13}$, and $K_A^E=u10^6\sim u10^{10}$, where u denotes the conversion coefficient for unit consistency ($u=5.6\times10^{18}\mathrm{IC}/(\mathrm{epitope}\times\mathrm{Ab})/\mathrm{M}^{-1}$). In contrast to the Fc$\gamma$RI/III mutant simulation, in this case, intact antibodies produced from plasma cells can mediate rapid clearance of antigens during the immune response.

As shown in Fig. 11A, the humoral immune response could be suppressed even by low-affinity intact antibody (e.g. $10^6\,M^{-1}$) due to rapid antigen clearance by phagocytotic cells. However, similar to the results from the FcγRI/III mutant simulation, only high-affinity $F(ab')_2$ (i.e., 10^9–$10^{10}\,M^{-1}$; Fig. 11C and D), which masked almost all epitopes (Fig. 8), could suppress the immune response. In every simulation, due to the faster decay of the $F(ab')_2$ fragments than SRBCs, the amount of unmasked epitopes increased with time. As shown in Fig. 11C, due to the exposure of epitopes once masked by $F(ab')_2$, activated B cells appeared between days 8 and 14. According to our simulations, intact antibody and $F(ab')_2$ did not result in different extents of epitope masking, but due to differences in the mediation of phagocytosis, there were substantial differences in the clearance profiles between SRBCs bound to $F(ab')_2$ and those bound to intact antibody.

5. Robustness analysis

The model developed for the simulation should produce consistent results even when the parameters listed in Table 2 and 4 are varied slightly. To explore the robustness of the model, we compared the results with those obtained using slightly different parameter values and with experimental data reported in the literature (Karlsson et al., 1999, 2001b).

The purpose of the model developed here was to predict antibody-induced immune suppression. The proliferation and death of B cells and the amount of administered

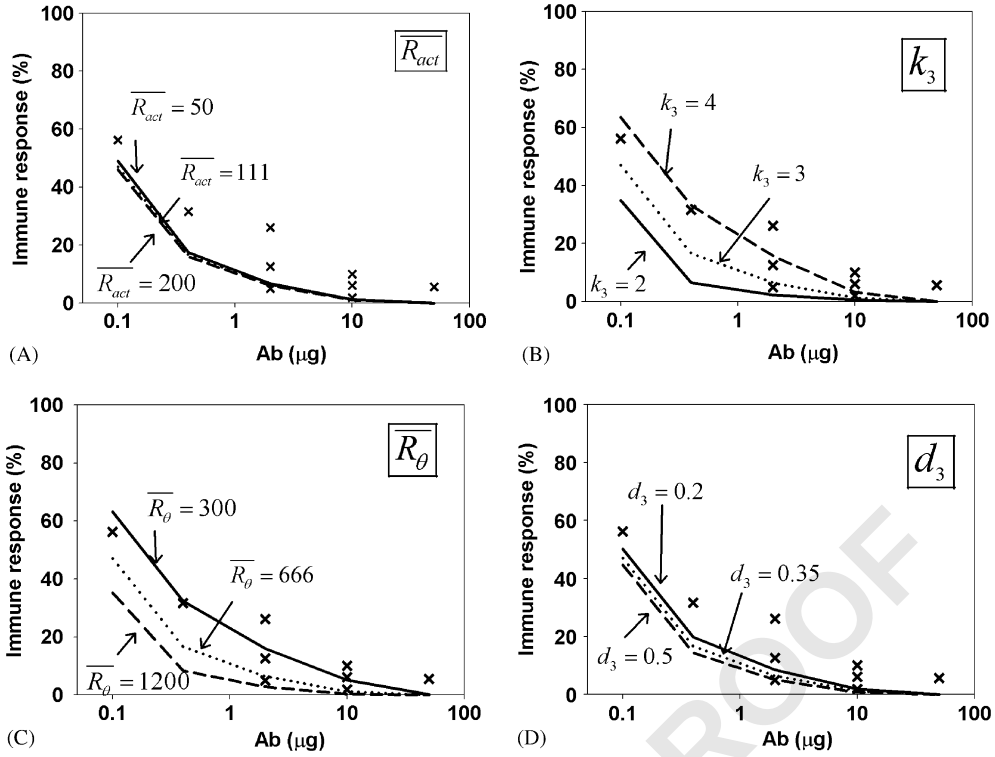

Fig. 12. Robustness of the model. Simulations were carried out with perturbed parameters and at $SRBC_{blood}(0) = 4 \times 10^6$ (4×10^6 SRBCs injected at time 0) and $Ab^E(0) = 4 \times 10^{12} - 2 \times 10^{15}$ (injection of 0.1–50 μg antibody [Ab] at time 0). The following parameters were perturbed: (A) the minimal number of epitope-BCR complexes per B-cell needed for activation ($\overline{R_{act}}$), (B) the rate constant for B-cell division (k_3), (C) the minimal number of epitope-BCR complexes per B-cell for survival ($\overline{R_\theta}$), and (D) the rate constant for B-cell apoptosis (d_3).

antibody are key factors that affect this model. Thus, we focused the validation on the parameters $\overline{R_{act}}$, k_3, $\overline{R_\theta}$, and d_3. The parameters were changed within the uncertainty range when it was known, but when it was not available, they were varied by approximately two-fold (Fig. 12). In each simulation, the amount of antibody was varied from 0.1 to 50 μg.

First, parameters influencing B-cell proliferation were examined. The minimum number of epitope-BCR complexes per B cell ($\overline{R_{act}}$) inversely influences the activation parameter (k_1) and controls B-cell activation. Despite large variations in $\overline{R_{act}}$, immune suppression was seldom affected because naïve B cells were completely depleted within 1 day (Fig. 4F). Thus $\overline{R_{act}}$ had little influence on immune suppression on day 5. The parameter k_3 controls the rate of B-cell division, and an increase in its value results in a rapid increase in the B-cell population. As a result, antibodies caused less immune suppression when k_3 was low. Because of exponential growth of the B-cell population, a two-fold change from $k_3 = 2$ to $k_3 = 4$ is expected to have a substantial effect on the suppression; however, it caused only an approximately two-fold difference in immune suppression.

Next, parameters influencing B-cell death were examined. There are three parameters that determine B-cell death rate: the rate of naïve B-cell death (d_1), the minimum number of BCR-epitope complexes for B-cell survival ($\overline{R_\theta}$), and the rate of B-cell apoptosis (d_3). Of these parameters, naïve B-cell death was not examined because it would not affect immune suppression significantly due to the rapid depletion of naïve B cells within 1 day. The two other parameters are the most important factors in our model because they determine the timing and the rate of B-cell death. As shown in Fig. 12C, the decrease of the $\overline{R_\theta}$ provides B cells with the ability to effectively resist cell death caused by antigen depletion. Consequently, the immune response was less suppressed when the survival threshold was decreased. Although the parameter was decreased by four-fold from $\overline{R_\theta} = 1200$ to $\overline{R_\theta} = 300$, the model still showed consistent results. The B-cell apoptosis rate parameter (d_3) also controls the B-cell population. Interestingly, in contrast to the $\overline{R_\theta}$, d_3 did not significantly influence the suppression. These results imply that B-cell death itself and not the rate of death is important in immune suppression.

These simulation results indicate that the model retains its robustness even when perturbed.

6. Discussion

In the present study, we developed a mathematical model to test the epitope masking hypothesis for immune suppression by passively administered antibodies. We simulated the typical immune response and immune suppression using parameters obtained from the literature or estimated based on physiological properties. The model

effectively reproduced the normal humoral immune response as well as the immune suppression, and the simulation results were in agreement with experimental findings.

In our model, at least 111 epitope-BCR complexes are required for B-cell activation. Interestingly, a low-affinity ($10^6\,M^{-1}$) antibody could also induce significant suppression even though it had a negligible masking effect—even at high concentrations, it could mask less than 20% of epitopes. Therefore, it appears that low-affinity antibodies cannot effectively mask epitopes and that the epitope masking hypothesis alone does not sufficiently explain the immune suppression caused by passive administration of low-affinity antibodies. Despite the insignificant effect of low-affinity antibodies on epitope-masking, as with high-affinity antibodies, SRBCs were cleared more rapidly when antibodies were administered than when they were not. Due to the rapid clearance of SRBCs, there was also a substantial reduction in epitope-BCR complexes for activation. Antibodies with an affinity of $10^6\,M^{-1}$ covered 2% of the epitopes on SRBCs, which means that approximately 20,000 antibody molecules were bound to each SRBC. The number of antibodies for half-maximal phagocytosis was approximately 11,000; thus, 2% occupancy was sufficient to induce a higher rate of phagocytosis. Although the $10^6\,M^{-1}$ antibody had little effect on epitope masking, it was sufficient to induce the rapid clearance of antigen. An antibody with affinity of $10^5\,M^{-1}$ masked less than 0.01% of the epitopes (~100 epitopes), which is less than the minimum number (400–1500) of antibodies required for mediation of phagocytosis (Miklós et al., 1993; Tolnay et al., 1992b). As a result, this antibody caused a less significant suppression than the $10^6\,M^{-1}$ antibody. In summary, higher affinity antibodies have a synergistic effect on immune suppression by causing both epitope masking and rapid clearance of antigen, whereas immune suppression by lower affinity antibodies is mediated solely by rapid antigen clearance.

In contrast to our results, it has been reported that the immune suppression is not affected by the loss of macrophage-mediated phagocytosis in the FcγRI/III knockout (Karlsson et al., 2001a). Thus, it is thought that antibody-mediated phagocytosis is not necessary for immune suppression in mice. To investigate the role of phagocytosis in immune suppression, we simulated the FcγRI/III mutant mouse model, wherein administered antibody could not facilitate phagocytosis. Due to the loss of phagocytosis, the administered antibodies did not affect antigen clearance but they did affect the immune response. High-affinity antibodies ($>10^8\,M^{-1}$) masked a majority of the epitopes so that B cells could not recognize and be activated by them. On the other hand, low-affinity antibodies ($10^6\,M^{-1}$) masked only 2% of epitopes so that the remaining 98% successfully induced a humoral immune response. There are two possible explanations for the difference between the simulation and experimental results. First, although in the reported mutant experiments, antigens were not eliminated by phagocytotic cells, antigens might be cleared by other mechanisms so that immune response was suppressed (Heyman, 2003). Second, in immune suppression experiments, antibodies were generally acquired from hyperimmunized mice (Heyman and Wigzell, 1984; Karlsson et al., 1999, 2001b), which means that the antibodies would have a higher affinity than those produced during the primary immune response. The immune response with the high-affinity antibodies from hyperimmunized mice seemed to suppress the immune response in the mutant mice to the same extent as found in the simulation with a $10^{10}\,M^{-1}$ antibody. Consequently, for low-affinity antibodies, rapid elimination of antigens, whether via phagocytotic cells or not, is important in immune suppression, whereas for high-affinity antibodies, epitope-masking alone is sufficient for immune suppression. Thus, we conclude that epitope masking and fast antigen clearance act synergistically in immune suppression.

We applied the model to simulate $F(ab')_2$ fragment-induced suppression, which has given conflicting experimental results. Due to the loss of the Fc part of the antibody, $F(ab')_2$ fragments can only mask epitopes and cannot mediate FcR-dependent B-cell inhibition. Therefore, it appears that the weak or absent immune suppression supports the FcR-mediated suppression hypothesis and contradicts the epitope masking hypothesis, although it has been reported that FcγRIIb knockout mice fail to show suppression of the immune response (Karlsson et al., 2001b). In brief, based on the $F(ab')_2$ experiments, the FcγRIIb receptor may be crucial for humoral immune suppression. Despite this interpretation, the different suppression phenomena may result not from the loss of FcγRIIb activation but rather from the decreased half-life of $F(ab')_2$ fragments, which also appears to support the epitope masking hypothesis. To test the effect of the $F(ab')_2$ half-life on immune suppression, we performed simulations in which the half-life was varied. We found that an increase in the half-life does not result in any significant suppression. Even an $F(ab')_2$ with a four-fold longer half-life than the intact antibody failed to suppress the immune response. These simulation results indicate that the shortened half-life of $F(ab')_2$ does not explain the conflicting results.

To further investigate why $F(ab')_2$ fragments cause a different degree of suppression than intact antibody, we performed simulations using $F(ab')_2$ with various affinities. We found that intact antibodies with an affinity of $10^8\,M^{-1}$ completely suppressed the humoral immune response, and even an antibody with an affinity of $10^6\,M^{-1}$ significantly suppressed the immune response. Injection of $F(ab')_2$ with affinities of 10^9 and $10^{10}\,M^{-1}$ also completely suppressed the immune response, but $F(ab')_2$ fragments with affinities below $10^8\,M^{-1}$ did not cause significant immune suppression. In particular, despite the same affinity, the $10^8\,M^{-1}$ $F(ab')_2$ and intact antibody caused completely different extents (negligible and complete, respectively) of immune

suppression. These simulation results are consistent with previously reported experimental results (Heyman, 1990). Furthermore, the complete immune suppression by both $F(ab')_2$ and intact antibody was also consistent with reported results (Cerottini et al., 1969; Karlsson et al., 1999; Tao and Uhr, 1966). According to our simulation results, the model effectively reproduced the $F(ab')_2$ experiments without incorporating FcγRIIb-mediated B-cell inhibition. Furthermore, the results of the model support those from the experimental knockout mice that FcγRIIb does not play important role in immune suppression (Karlsson et al., 1999).

To better understand $F(ab')_2$-induced immune suppression, we determined the percentage of masked epitopes and SRBCs in the spleen. The epitope-masking effect of $F(ab')_2$ and intact antibody did not differ significantly, but, especially at affinities of 10^9 and $10^{10}\,M^{-1}$, they resulted in very different profiles of SRBC degradation. Because of loss of the Fc portion, $F(ab')_2$ could not facilitate SRBC clearance so that the SRBCs persisted much longer than in the normal response. Nonetheless, the fragments masked a majority of epitopes on the SRBCs, which prevented B-cell activation. Interestingly, after day 8, an immune response was evoked as a result of increased exposure of masked epitopes due to the shorter half-life of the $F(ab')_2$ fragments than the SRBCs. This delayed immune response has not been previously reported, possibly because PFCs were measured on day 5, which could preclude the observation of a delayed response. Therefore, this prediction remains to be verified experimentally.

Consequently, the simulation results explain the apparently conflicting results. It seems that the different suppression profiles by $F(ab')_2$ and intact antibody are not due to the decreased half-life of $F(ab')_2$ or the loss of FcγRIIb-dependent B-cell inhibition. Rather, the different profiles are due to the loss of the antibody's ability to mediate phagocytosis because the Fc portion is necessary not only for FcγRIIb-dependent B-cell inhibition but also for FcγRI/III-dependent phagocytosis. In summary, we suggest that the conflicting results produced by $F(ab')_2$ fragments can be explained by a combination of the epitope masking and rapid clearance hypotheses.

7. Conclusion

The epitope masking hypothesis for immune suppression by passively administered antibodies is difficult to prove experimentally. Therefore, we developed a mathematical model of immune suppression to test this hypothesis. Using this model, we found that generally accepted interpretations might not be true, including the irrelevance of FcγRI/III receptor, the role of the decreased half-life of $F(ab')_2$, and the involvement of the FcγRIIb receptor. In addition, the model indicated that immune suppression is strongly affected by the antibody affinity, an aspect generally not considered in the design and interpretation of experiments. Thus, our results emphasize that antibody affinity should be considered before carrying out experiments. Although our model is mathematical, these results provide new insight into how passively administered antibodies induce immune suppression.

Our model effectively reproduced immune suppression phenomena, but it did not consider steric hindrance between antibodies. Because antibodies are much larger than epitopes, epitope-bound antibody could interfere with the interaction of nearby epitopes and antibodies. This is an important consideration if two additional epitopes are present and the epitope densities are very high. In such cases, the model needs to be modified for better predictability; however, this is easily done because the model considers individual epitope interactions.

Acknowledgments

This work was supported by a National Research Laboratory Grant (2005-01450) from the Ministry of Science and Technology, Korea.

Appendix A

Four different proteins in our model can bind epitopes: BCRs, secreted antibodies, administered antibodies, and administered $F(ab')_2$ fragments. Among these, the secreted antibodies and BCRs have the same affinities because they have identical epitope-binding regions. In addition, in the simulations, extrinsic antibodies and $F(ab')_2$ fragments are not administered at the same time; thus, for simplicity, two new variables were assigned: $Ab_1 = Ab^I + R(B^*)$ and $Ab_2 = Ab^E + F_{ab}$, where Ab^I denotes the total number of antibodies produced by plasma cells, $R(B^*)$ is the total number of BCRs, Ab^E is the number of administered antibodies, and F_{ab} is the number of administered $F(ab')_2$ fragments. It should be noted that, although the variable Ab_2 is the sum of the administered antibodies and $F(ab')_2$ fragments, due to the exclusive administration condition, one of the terms can be ignored depending on the simulation conditions; however, for consistency of the model, this term was assigned. For the two imaginary antibodies (Ab_1 and Ab_2), the following equilibrium reactions were considered:

$$Ab_1 + Ag \underset{v_{-1}}{\overset{v_1}{\rightleftharpoons}} C_1,$$

$$Ab_2 + Ag \underset{v_{-2}}{\overset{v_2}{\rightleftharpoons}} C_2,$$

$$\frac{dAb_1}{dt} = -v_1 Ab_2 Ag + v_{-1} C_1, \tag{A.1}$$

$$\frac{dAb_2}{dt} = -v_2 Ab_2 Ag + v_{-2} C_2, \tag{A.2}$$

where $K_A^I = v_1/v_{-1}$ and $K_A^E = v_2/v_{-2}$ denotes the affinities of Ab_1 and Ab_2, respectively; C_1 and C_2 are the corresponding immune complexes; and Ag denotes the

total number of epitopes on SRBCs. The differential equations (A.1) and (A.2) were resolved as follows:

$$g(Ag_{free}) = \alpha Ag_{free}^3 + (\beta - \alpha\Delta)Ag_{free}^2 + (1 - \beta\Delta - Ab_1^0 K_A^E - Ab_2^0 K_A^I)Ag_{free} - Ag^0 = 0, \quad (A.3)$$

$$g(Ag_{free})' = 3\alpha Ag_{free}^2 + 2(\beta - \alpha\Delta)Ag_{free} + (1 - \beta\Delta - Ab_1^0 K_A^E - Ab_2^0 K_A^I) = 0, \quad (A.4)$$

where $\alpha = K_A^I K_A^E$, $\beta = K_A^I + K_A^E$ and $\Delta = Ag^0 - Ab_1^0 - Ab_2^0$. Ag_{free} denotes free epitopes at equilibrium; Ag^0 the initial number of epitopes; and Ab_1^0 and Ab_2^0 denote the initial number of plasma cell-produced antibodies plus BCRs and administered antibodies or F(ab′)$_2$ fragments, respectively. Because $g(0)<0$, Eq. (A.3) has at least one positive solution. In addition, the derivative of the Eq. (A.4) has one negative and one positive solution if the condition $1 - \beta\Delta - Ab_1^0 K_A^E - Ab_2^0 K_A^I < 0$ is satisfied. $1 - \beta\Delta - Ab_1^0 K_A^E - Ab_2^0 K_A^I > 0$ is satisfied only when almost all molecules are removed ($Ag \approx Ab_1^0 \approx Ab_2^0 \approx 0$), in other words, when the immune response has been completely over. This condition, however, is not considered in our simulations so that we obtain only one positive solution for the number of free epitopes.

The number of each imaginary antibody can be obtained through the calculation process. The ratio of epitope-BCR complexes to epitope-antibody complexes is proportional to that of the BCR to antibody ratio. Hence, the epitope-antibody complex (IC^I) and the epitope-BCR complex per B cell ($\overline{R_{bound}}$) can be obtained from Eqs. (A.5) and (A.7). The epitope-antibody complexes per SRBC ($\overline{IC^I}$) can also be calculated by dividing (A.5) by the number of SRBCs in the blood and spleen (A.6).

$$IC^I = \frac{Ab^I}{Ab^I + R_T} C_1, \quad (A.5)$$

$$\overline{IC^I} = \frac{IC^I}{S_{blood} + S_{spleen}}, \quad (A.6)$$

$$\overline{R_{bound}} = \frac{R_T}{Ab^I + R_T} C_1 \frac{1}{B^*}, \quad (A.7)$$

where $B^* = B_N + \sum_{i=0}^{10} B_i$ and $R_T = bB^*$.

Likewise, the complex of epitope and administered antibody (IC^E) and the complex of epitope and F(ab′)$_2$ fragment ($IC^{F_{ab}}$) can be calculated. The numbers per SRBC, $\overline{IC^E}$ and $\overline{IC^{F_{ab}}}$, can also be obtained.

$$IC^E = \frac{Ab^E}{Ab^E + F_{ab}} C_2, \quad (A.8)$$

$$\overline{IC^E} = \frac{IC^E}{S_{blood} + S_{spleen}}, \quad (A.9)$$

$$IC^{F_{ab}} = \frac{F_{ab}}{Ab^E + F_{ab}} C_2, \quad (A.10)$$

$$\overline{IC^{F_{ab}}} = \frac{IC^{F_{ab}}}{S_{blood} + S_{spleen}}. \quad (A.11)$$

Consequently, the number of bound antibodies per SRBC ($\overline{Ab_{bound}} = \overline{IC^I} + \overline{IC^E}$), which can mediate phagocytosis, can also be calculated. Because of the inability to mediate phagocytosis, the term $\overline{IC^{F_{ab}}}$ is not added to $\overline{Ab_{bound}}$.

Appendix B

The number of epitope-BCR complexes (R_{act}) can be calculated using equilibrium kinetics of the BCR- and epitope-binding reaction as shown in (B.1) (see Table 4 for a detailed description of parameters). By solving Eq. (B.1), we obtained Eq. (B.2):

$$K_A^I = \frac{R_{act}}{(e_0 - R_{act})(R_0 - R_{act})}, \quad (B.1)$$

$$f(R_{act}) = R_{act}^2 - \left(e_0 + R_0 + \frac{1}{K_A^I}\right) R_{act} + e_0 R_0 = 0. \quad (B.2)$$

By simple algebra, Eq. (B.2) can be shown to have two positive solutions. Because $f(e_0)<0$ and $f(R_0)<0$, the larger of the two solutions is always larger than e_0 and R_0 so that the larger solution is unphysical. By dividing the smaller solution by the number of naïve B cells, we obtain the number of BCR-epitope complexes per B cell required for stimulation (B.3).

$$\overline{R_{act}} = \frac{e_0 + R_0 + 1/K_A^I - \sqrt{(e_0 + R_0 + 1/K_A^I)^2 - 4e_0 R_0}}{2} \frac{1}{B_N^0}. \quad (B.3)$$

References

Adler, F.L., 1965. Studies on mouse antibodies. I. The response to sheep red cells. J. Immunol. 95 (1), 26–38.

Aggarwal, A., Catlett, J.P., 2002. Rituximab: an anti-CD20 antibody for the treatment of chronic refractory immune thrombocytopenic purpura. South. Med. J. 95 (10), 1209–1212.

Agrawal, N.G.B., Linderman, J.J., 1996. Mathematical modeling of helper T lymphocyte/antigen-presenting cell interactions: analysis of methods for modifying antigen processing and presentation. J. Theor. Biol. 182 (4), 487–504.

Anderson, C.F., Gerber, J.S., Mosser, D.M., 2002. Modulating macrophage function with IgG immune complexes. J Endotoxin Res 8 (6), 477–481.

Andersson, J., Coutinho, A., Lernhardt, W., Melchers, F., 1977. Clonal growth and maturation to immunoglobulin secretion in vitro of every growth-onducible B lymphocytes. Cell 10, 27–34.

Ashman, R.F., Peckham, D., Stunz, L.L., 1996. Fc receptor off-signal in the B cell involves apoptosis. J. Immunol. 157 (1), 5–11.

Bachmann, M.F., Kundig, T.M., Kalberer, C.P., Hengartner, H., Zinkernagel, R.M., 1994. How many specific B cells are needed to protect against a virus? J. Immunol. 152 (9), 4235–4241.

Barnes, N., Gavin, A.L., Tan, P.S., Mottram, P., Koentgen, F., Hogarth, P.M., 2002. FcγRI-deficient mice show multiple alterations to inflammatory and immune responses. Immunity 16 (3), 379–389.

Beck, K., 1981. A mathematical model of T-cell effects in the humoral immune response. J. Theor. Biol. 89 (4), 593–610.

Bell, G.I., 1970a. Mathematical model of clonal selection and antibody production. J. Theor. Biol. 29 (2), 191–232.

Bell, G.I., 1970b. Mathematical model of clonal selection and antibody production. Nature 228 (5273), 739–744.

Bell, G.I., 1971a. Mathematical model of clonal selection and antibody production III. The cellular basis of immunological paralysis. J. Theor. Biol. 33 (2), 379–398.

Bell, G.I., 1971b. Mathematical model of clonal selection and antibody production. II. J. Theor. Biol. 33 (2), 339–378.

Bezdicek, P., Worgall, S., Kovesdi, I., Kim, M.-K., Park, J.-G., Vincent, T., Leopold, P.L., Schreiber, A.D., Crystal, R.G., 1999. Enhanced liver uptake of opsonized red blood cells after in vivo transfer of fcgamma RIIA cDNA to the Liver. Blood 94 (10), 3448–3455.

Bocharov, G.A., Romanyukha, A.A., 1994. Mathematical model of antiviral immune response III. Influenza a virus infection. J. Theor. Biol. 167 (4), 323–360.

Bourget, I., Di Berardino, W., Breittmayer, J.P., Grenier-Brossette, N., Plana-Prades, M., Bonnefoy, J.Y., Cousin, J.L., 1995. CD20 monoclonal antibodies decrease interleukin-4stimulated expression of the low-affinity receptor for IgE (Fc epsilon RII/CD23) in human B cells by increasing the extent of its cleavage. Eur. J. Immunol. 25 (7), 1872–1876.

Brauweiler, A., Tamir, I., Marschner, S., Helgason, C.D., Cambier, J.C., 2001. Partially distinct molecular mechanisms mediate inhibitory FcγRIIB signaling in resting and activated B cells. J. Immunol. 167 (1), 204–211.

Brüggemann, M., Rajewsky, K., 1982. Regulation of the antibody response against hapten-coupled erythrocytes by monoclonal anti-hapten antibodies of various isotypes. Cell. Immunol. 71 (2), 365–373.

Calame, K.L., Lin, K.-I., Tunyaplin, C., 2003. Regulatory mechanisms that determine the development and function of plasma cells. Annu. Rev. Immunol. 21 (1), 205–230.

Cambier, J.C., 1995. Antigen and Fc receptor signaling. The awesome power of the immunoreceptor tyrosine-based activation motif (ITAM). J. Immunol. 155 (7), 3281–3285.

Cartwright, J.H.E., Piro, O., 1992. The Dynamics of Runge–Kutta Methods. Int. J. Bifurc. Chaos 2, 427–449.

Cerottini, J.C., McConahey, P.J., Dixon, F.J., 1969. The immunosuppressive effect of passively administered antibody IgG fragments. J. Immunol. 102 (4), 1008–1015.

Chilcott, J., Jones, M.L., Wight, J., Forman, K., Wray, J., Beverley, C., Tappenden, P., 2003. A review of the clinical effectiveness and cost-effectiveness of routine anti-D prophylaxis for pregnant women who are rhesus-negative. Health Technol. Assess. 7 (4).

Clarke, C.A., Donohoe, W.T., Mc, C.R., Woodrow, J.C., Finn, R., Krevans, J.R., Kulke, W., Lehane, D., Sheppard, P.M., 1963. Further experimental studies on the prevention of Rh haemolytic disease. Br. Med. J. 5336, 979–984.

Cozine, C.L., Wolniak, K.L., Waldschmidt, T.J., 2005. The primary germinal center response in mice. Current Opinion in Immunology 17 (3), 298–302.

Donahue, A.C., Fruman, D.A., 2003. Proliferation and survival of activated B cells requires sustained antigen receptor engagement and phosphoinositide 3-kinase activation. J. Immunol. 170 (12), 5851–5860.

Enriquez-Rincon, F., Klaus, G.G., 1984. Differing effects of monoclonal anti-hapten antibodies on humoral responses to soluble or particulate antigens. Immunology 52 (1), 129–136.

Finn, R., Clarke, C.A., Donohow, W.T., McConnell, R.B., Sheppard, P.M., Lehane, D., Kulke, W., 1961. Experimental studies on the prevention of Rh haemolytic disease. Br. Med. J. 1, 1486–1490.

Fulcher, D.A., Basten, A., 1997. B cell life span: a review. Immunol. Cell. Biol. 75 (5), 446–455.

Funk, G.A., Barbour, A.D., Hengartner, H., Kalinke, U., 1998. Mathematical model of a virus-neutralizing immunglobulin response. J. Theor. Biol. 195 (1), 41–52.

Golay, J., Zaffaroni, L., Vaccari, T., Lazzari, M., Borleri, G.-M., Bernasconi, S., Tedesco, F., Rambaldi, A., Introna, M., 2000. Biologic response of B lymphoma cells to anti-CD20 monoclonal antibody rituximab in vitro: CD55 and CD59 regulate complement-mediated cell lysis. Blood 95 (12), 3900–3908.

Guo, T.L., McCay, J.A., Brown, R.D., Musgrove, D.L., Germolec, D.R., Butterworth, L., Munson, A.E., White Jr., K.L., 2000. Carbon tetrachloride is immunosuppressive and decreases host resistance to Listeria monocytogenes and Streptococcus pneumoniae in female B6C3F1 mice. Toxicology 154 (1–3), 85–101.

Guzman-Rojas, L., Sims-Mourtada, J.C., Rangel, R., Martinez-Valdez, H., 2002. Life and death within germinal centres: a double-edged sword. Immunology 107 (2), 167–175.

Han, S., Zheng, B., Takahashi, Y., Kelsoe, G., 1997. Distinctive characteristics of germinal center B cells. Seminar. Immunol. 9 (4), 255–260.

Henry, C., Jerne, N.K., 1968. Competition of 19S and 7S antigen receptors in the regulation of the primary immune response. J. Exp. Med. 128 (1), 133–152.

Heyman, B., 1990. Fc-dependent IgG-mediated suppression of the antibody response: fact or Artifact? Scand. J. Immunol. 31, 601–607.

Heyman, B., 2003. Feedback regulation by IgG antibodies. Immunol. Lett. 88 (2), 157–161.

Heyman, B., Wigzell, H., 1984. Immunoregulation by monoclonal sheep erythrocyte-specific IgG antibodies: suppression is correlated to level of antigen binding and not to isotype. J. Immunol. 132 (3), 1136–1143.

Heyman, B., Dahlström, J., Diaz de Ståhl, T., Getahun, A., Wernersson, S., Karlsson, M.C.I., 2001. No evidence for a role of Fc RIIB in suppression of in vivo antibody responses to erythrocytes by passively administered IgG. Scand. J. Immunol. 53 (4), 331–334.

Hodgkin, P.D., Lee, J.H., Lyons, A.B., 1996. B cell differentiation and isotype switching is related to division cycle number. J. Exp. Med. 184 (1), 277–281.

Jhagvaral Hasbold, A.B.L.M.R.K.P.D.H., 1998. Cell division number regulates IgG1 and IgE switching of B cells following stimulation by CD40 ligand and IL-4. Eur. J. Immunol. 28 (03), 1040–1051.

Junghans, R.P., Anderson, C.L., 1996. The protection receptor for IgG catabolism is the beta 2-microglobulin-containing neonatal intestinal transport receptor. Proc. Natl. Acad. Sci. USA 93 (11), 5512–5516.

Karlsson, M.C.I., Wernersson, S., Diaz de Ståhl, T., Gustavsson, S., Heyman, B., 1999. Efficient IgG-mediated suppression of primary antibody responses in Fcγ receptor-deficient mice. Proc. Natl. Acad. Sci. USA 96 (5), 2244–2249.

Karlsson, M.C.I., Diaz de Ståhl, T., Heyman, B., 2001a. IgE-mediated suppression of primary antibody responses in vivo. Scand. J. Immunol. 53 (4), 381–385.

Karlsson, M.C.I., Getahun, A., Heyman, B., 2001b. FcγRIIB in IgG-mediated suppression of antibody responses: different impact in vivo and in vitro. J. Immunol. 167 (10), 5558–5564.

Keşmir, C., De Boer, R.J., 1999. A mathematical model on germinal center kinetics and termination. J. Immunol. 163 (5), 2463–2469.

Kettman, J., Dutton, R.W., 1970. An in vitro primary immune response to 2,4,6-trinitrophenyl substituted erythrocytes: response against carrier and hapten. J. Immunol. 104 (6), 1558–1561.

Kevin Hollowood, J.R.G., 1998. Germinal centre cell kinetics. J. Pathol. 185 (3), 229–233.

Kimoto, H., Nagaoka, H., Adachi, Y., Mizuochi, T., Azuma, T., Yagi, T., Sata, T., Yonehara, S., Tsunetsugu-Yokota, Y., Taniguchi, M., Takemori, T., 1997. Accumulation of somatic hypermutation and antigen-driven selection in rapidly cycling surface Ig+ germinal center

(GC) B cells which occupy GC at a high frequency during the primary anti-hapten response in mice. Eur. J. Immunol. 27 (1), 268–279.

Kracker, S., Radbruch, A., 2004. Immunoglobulin class switching: in vitro induction and analysis. Methods Mol. Biol. 271, 149–159.

Kumpel, B.M., 2002. On the mechanism of tolerance to the Rh D antigen mediated by passive anti-D (Rh D prophylaxis). Immunol. Lett. 82 (1–2), 67–73.

Kumpel, B.M., Elson, C.J., 2001. Mechanism of anti-D-mediated immune suppression—a paradox awaiting resolution? Trends Immunol. 22 (1), 26–31.

Kumpel, B.M., Goodrick, M.J., Pamphilon, D.H., Fraser, I.D., Poole, G.D., Morse, C., Standen, G.R., Chapman, G.E., Thomas, D.P., Anstee, D.J., 1995. Human Rh D monoclonal antibodies (BRAD-3 and BRAD-5) cause accelerated clearance of Rh D+ red blood cells and suppression of Rh D immunization in Rh D-volunteers. Blood 86 (5), 1701–1709.

Leanderson, T., Kallberg, E., Gray, D., 1992. Expansion, selection and mutation of antigen-specific B cells in germinal centers. Immunol. Rev. 126, 47–61.

Lee, S.H., Starkey, P.M., Gordon, S., 1985. Quantitative analysis of total macrophage content in adult mouse tissues. Immunochemical studies with monoclonal antibody F4/80. J. Exp. Med. 161 (3), 475–489.

Liu, Y.J., Zhang, J., Lane, P.J., Chan, E.Y., MacLennan, I.C., 1991. Sites of specific B cell activation in primary and secondary responses to T cell-dependent and T cell-independent antigens. Eur. J. Immunol. 21 (12), 2951–2962.

Maclennan, I.C.M., 1994. Germinal Centers. Ann. Rev. Immunol. 12 (1), 117–139.

McHeyzer-Williams, L.J., Driver, D.J., McHeyzer-Williams, M.G., 2001. Germinal center reaction. Curr. Opin. Hematol. 8 (1), 52–59.

Melchers, F., Andersson, J., 1986. Factors controlling the B-cell cycle. Ann. Rev. Immunol. 4 (1), 13–34.

Merrill, S.J., 1978a. A model of the stimulation of B-cells by replicating antigen—I. Math. Biosci. 41 (1-2), 125–141.

Merrill, S.J., 1978b. A model of the stimulation of B-cells by replicating antigen–II. Math. Biosci. 41 (1–2), 143–156.

Merrill, S.J., 1998. Computational models in immunological methods: an historical review. J. Immunol. Methods 216 (1–2), 69–92.

Miklós, K., Tolnay, M., Bazin, H., Medgyesi, G.A., 1992. Antibody mediated lysis of hapten-conjugated target cells by macrophages and by complement: the influence of IgG subclass, antibody and hapten density. Mol. Immunol. 29 (3), 379–384.

Miklós, K., Tolnay, M., Bazin, H., Medgyesi, G.A., 1993. Rat IgG subclasses mediating binding and phagocytosis of target cells by homologous macrophages. Mol. Immunol. 30 (14), 1273–1278.

Mohr, M., Kolb, H., Kolb-Bachofen, V., Schlepper-Schafer, J., 1987. Recognition of xenogeneic erythrocytes: the GalNAc/Gal-particle receptor of rat liver macrophages mediates or participates in recognition. Biol. Cell 60 (3), 217–224.

Moise Jr., K.J., 2002. Management of rhesus alloimmunization in pregnancy. Obstet. Gynecol. 100 (3), 600–611.

Möller, G., Wigzell, H., 1965. Antibody synthesis at the cellular level. Antibody-induced suppression of 19S and 7S antibody response. J. Exp. Med. 121 (6), 969–989.

Naito, M., Hasegawa, G., Takahashi, K., 1997. Development, differentiation, and maturation of Kupffer cells. Microsc. Res. Techn. 39 (4), 350–364.

Ouchi, E., Seiji, K., Sato, J., Nomura, N., Watabe, S., 1976. Erythrocyte rosette forming activity of macrophage. Tohoku J. Exp. Med. 118 (Suppl), 199–205.

Pierre, D.M., Goldman, D., Bar-Yam, Y., Perelson, A.S., 1997. Somatic evolution in the immune system: the need for germinal centers for efficient affinity maturation. J. Theor. Biol. 186 (2), 159–171.

Pittner, B.T., Snow, E.C., 1998. Strength of signal through BCR determines the fate of cycling B cells by regulating the expression of the Bcl-2 family of survival proteins. Cell. Immunol. 186 (1), 55–62.

Quintana, I.Z., Silveira, A.V., Möller, G., 1987. Regulation of the antibody response to sheep erythrocytes by monoclonal IgG antibodies. Eur. J. Immunol. 17, 1343–1349.

Rathmell, J.C., 2004. B-cell homeostasis: digital survival or analog growth? Immunolog. Rev. 197 (1), 116–128.

Ravetch, J.V., Lanier, L.L., 2000. Immune inhibitory receptors. Science 290 (5489), 84–89.

Reth, M., Hombach, J., Wienands, J., Campbell, K.S., Chien, N., Justement, L.B., Cambier, J.C., 1991. The B-cell antigen receptor complex. Immunol. Today 12 (6), 196–201.

Rihova, B., Vetvicka, V., 1984. Uptake of ^{51}Cr-SRBC in low- and high-responder mouse strains. Folia Biol. (Praha) 30 (1), 57–66.

Rosado, M.M., Freitas, A.A., 1998. The role of the B cell receptor V region in peripheral B cell survival. Eur. J. Immunol. 28 (09), 2685–2693.

Rundell, A., DeCarlo, R., HogenEsch, H., Doerschuk, P., 1998. The humoral immune response to haemophilus influenzaetype b: a mathematical model based on T-zone and germinal center B-cell dynamics. J. Theor. Biol. 194 (3), 341–381.

Sármay, G., Koncz, G., Pecht, I., Gergely, J., 1999. Cooperation between SHP-2, phosphatidyl inositol 3-kinase and phosphoinositol 5-phosphatase in the FcγRIIb mediated B cell regulation. Immunol. Lett. 68 (1), 25–34.

Smith, S.H., Reth, M., 2004. Perspectives on the nature of BCR-mediated survival signals. Mol. Cell 14 (6), 696–697.

Strasser, A., Whittingham, S., Vaux, D.L., Bath, M.L., Adams, J.M., Cory, S., Harris, A.W., 1991. Enforced BCL2 expression in B-lymphoid cells prolongs antibody responses and elicits autoimmune disease. Proc. Natl. Acad. Sci. USA 88 (19), 8661–8665.

Tao, T.-W., Uhr, J.W., 1966. Capacity of pepsin-digested antibody to inhibit antibody formation. Nature 212, 208–209.

Tarlinton, D., 1998. Germinal centers: form and function. Curr. Opin. Immunol. 10 (3), 245–251.

Tolnay, M., Miklós, K., Bazin, H., Medgyesi, G.A., 1992a. Interaction between rat peritoneal macrophages and sensitised erythrocytes: dependence on IgG subclass, antibody density and the degree of hapten conjugation. Mol. Immunol. 29 (3), 385–390.

Tolnay, M., Miklós, K., Bazin, H., Medgyesi, G.A., 1992b. Interaction between rat peritoneal macrophages and sensitised erythrocytes: dependence on IgG subclass, antibody density and the degree of hapten conjugation. Mol. Immunol. 29 (3), 385–390.

van Rijen, E.A.M., Ward, J.J., Little, R.A., 1998. Effects of colloidal resuscitation fluids on Reticuloendothelial function and resistance to infection after hemorrhage. Clin. Diagn. Lab. Immunol. 5 (4), 543–549.

Waltman, P., Butz, E., 1977. A threshold model of antigen-antibody dynamics. J. Theor. Biol. 65 (3), 499–512.

Warren, D.S., Zachary, A.A., Sonnenday, C.J., King, K.E., Cooper, M., Ratner, L.E., Sue Shirey, R., Haas, M., Leffell, M.S., Montgomery, R.A., 2004. Successful renal transplantation across simultaneous ABO incompatible and positive crossmatch barriers. Am. J. Transplant. 4 (4), 561–568.

Wilson, P.C., Bouteiller, O.d., Liu, Y.-J., Potter, K., Banchereau, J., Capra, J.D., Pascual, V., 1998. Somatic hypermutation introduces insertions and deletions into immunoglobulin V genes. J. Exp. Med. 187 (1), 59–70.

Woodrow, J.C., Clarke, C.A., Donohow, W.T., Finn, R., McConnell, R.B., Sheppard, P.M., Lehane, D., Roberts, F.M., Gimlette, T.M., 1975. Mechanism of Rh prophylaxis: an experimental study on specificity of immunosuppression. Br. Med. J. 2, 57–59.

Yoshii, H., Fukata, Y., Yamamoto, K., Yago, H., Suehiro, S., Yanagihara, Y., Okudaira, H., 1996. A new assay system detecting antibody production and delayed-type hypersensitivity responses to trinitrophenyl hapten in an individual mouse. Int. J. Immunopharmaco. 18 (1), 31–36.